

# MICROCOLUMN CHROMATOGRAPHY

DAIDO ISHII, MASASHI GOTO, TOYOHIDE TAKEUCHI,  
and AKIO HIROSE

*Department of Applied Chemistry*

(Received April 12, 1989)

## Abstract

Miniaturization of the separation column produces numerous merits in high-performance liquid chromatography (HPLC). The attractive features of micro-HPLC are demonstrated by various applications, in which laboratory-made instruments are employed. Microcolumn-based detection showed versatility and better mass sensitivity of micro-HPLC. The micro-HPLC system is applicable to gas chromatography and supercritical fluid chromatography, leading to unification of chromatography.

## Contents

1. Brief history of micro-HPLC .....	2
2. Attractive features of micro-HPLC .....	2
3. Instrumentation .....	4
3.1. Pumping system .....	4
3.2. Injection system .....	4
3.3. Column preparation .....	6
3.4. Detection system .....	6
4. Applications .....	8
4.1. Catecholamines and their metabolites .....	8
4.2. Bile acids .....	10
4.3. Amino acids .....	10
4.4. Proteins .....	14
4.5. Industrial chemicals .....	15
5. Microcolumn-based detection .....	17
5.1. Direct combination with FABMS .....	18
5.2. On-column detection .....	21
5.3. Indirect detection .....	24
6. Open-tubular capillary LC .....	27
6.1. Theoretical aspects .....	27
6.2. Performance of open-tubular columns .....	29

7. Approach to SFC and GC: Unified chromatography .....	32
8. Future prospects of microcolumn chromatography .....	36

## 1. Brief history of micro-HPLC

Chromatography was named by Tswett and its definition was provided in his paper in 1906.<sup>1)</sup> The name referred to separation of coloured bands in a column and was composed of two Greek words, *chroma*-colour and *graphein*-write. He found in the work that when a petroleum ether solution of chlorophyll was filtered through a column of adsorbent, the pigments were deposited in separate coloured zones along the column from the top to the bottom. Tswett is generally considered as the originator of this field. As a matter of fact, however, the phenomena based on chromatography were realized earlier than his discovery. For example, Day<sup>2)</sup> purified petroleum by using a limestone such as the Trenton limestone in 1897. At any rate, nature itself has been using chromatography to provide us enriched layers of minerals and purified petroleum fractions.

Since the discovery of adsorption chromatography various types of chromatography methods were invented. The origin of paper, thin-layer and ion-exchange chromatography go back to the 1930's, gas chromatography (GC) and gel chromatography to the 1950's, and supercritical fluid chromatography (SFC) to 1960's. In the last two decades high-performance liquid chromatography (HPLC) and open-tubular capillary GC have remarkably advanced.

In HPLC 4–6 mm ID columns packed with 3–30  $\mu\text{m}$  materials have been usually employed. Researches on miniaturization of the column dimension in liquid chromatography (LC) were started at the same time as the birth of HPLC. Horváth et al.<sup>3)</sup> introduced their pellicular packings for use in LC in 1967 and used columns one meter long, 0.5 and 1.0 mm ID, packed with those pellicular packings. Scott and Kucera<sup>4)</sup> published a paper in 1976, in which they used 1 mm ID columns. Ishii's group<sup>5)</sup> started researches on miniaturization in HPLC in the early 1970's.

Interests in micro-HPLC gradually increased since the introduction, and microcolumns are now commercially available from a number of manufacturers. On August 25–28, 1982, thirty-two experts from Japan and the United States, joined by four participants from other countries, met in Hawaii to discuss advances in the field of microcolumn separation methods. That was the first international meeting on micro-HPLC. Comprehensive information on micro-HPLC and its state of the art are given in several published books.<sup>6)-9)</sup>

## 2. Attractive features of micro-HPLC

Before describing the features of micro-HPLC, it seems inevitable to define the column dimension as well as the column type employed in micro-HPLC. Micro-HPLC columns can generally be divided into three categories according to their packing states: (1) densely packed columns; (2) loosely packed columns; and (3) open-tubular columns. The first type is usually employed in HPLC. The densely packed columns can be divided, according to the column diameter, into three categories: conventional HPLC, semi-micro-HPLC, and micro-HPLC.

Table 1 lists typical column dimensions of these densely packed columns and compares them with those of loosely packed and open-tubular columns. Semi-micro-HPLC covers

Table 1. Typical dimensions of HPLC columns.

Category	ID (mm)	Reciprocal of Relative cross-sectional area
Densely packed columns		
Conventional HPLC	4–6	1.3–0.59
Semi-micro-HPLC	1–2	21–5.3
Micro-HPLC	0.2–0.5	530–85
Loosely packed column	0.05–0.2	8,500–530
Open-tubular column	0.01–0.05	210,000–8,500

columns with 1 to 2-mm i.d. and packed microbore columns (initiated by Horváth<sup>3)</sup> and Scott<sup>4)</sup>) are included in this category. The reciprocal of the relative cross-sectional area of the various column types, compared with the 4.6-mm ID column (which is the most common in HPLC), is also indicated in Table 1. Generally speaking, the column volume of micro-HPLC columns is less than one-hundredth of that of conventional HPLC columns. The separation column in this article generally refers to the densely packed column unless otherwise specified.

Attractive features of micro-HPLC can be naturally generated by employing small-diameter columns. We can expect the following advantages from micro-HPLC:

1. Low consumption of both mobile and stationary phases, which facilitates the use of exotic or expensive phases;
2. Increase in mass sensitivity;
3. Achievement of high resolution with long columns;
4. Easy control of column temperature;
5. Convenience of selecting the operating conditions;
6. Convenience of coupling with mass spectrometry (MS).

The decrease in the column diameter leads to low consumption of the stationary phase, which facilitates the use of valuable and expensive packing materials or long columns. It also leads to operation at lower flow rates when the linear velocity is kept constant independent of the column diameter, which in turn leads to low consumption of the mobile phase. A large volume of the mobile phase and various types of separation columns are needed to establish the optimum operating conditions for the analysis of new samples, leading to an increased waste of solvents. Micro-HPLC is also convenient for analysis of new samples and several milliliters of solvent is enough to optimize the mobile phase conditions in micro-HPLC.

The peak volume is generally proportional to the column volume provided that the same column efficiency (or theoretical plate number) is achieved independent of the column dimension. Therefore, the decrease in the column volume compels us to use a small-volume detection system so that the column efficiency should not be deteriorated during the detection process. If the concentration sensitivity of the miniaturized detection system is maintained, the mass sensitivity can be improved by a factor of the ratio of the peak volumes. The increase in the mass sensitivity is especially important when dealing with the separation and analysis of samples of biological origin. Such samples often contain very limited quantities of the individual solutes to be separated.

Reasonable theoretical plates, with respect to column length, can be attained as a result of the decreased multi-path diffusion and effective transfer of heat generated by the pressure drop. The heat generated in the column affects the mass-transfer processes and produces poor column efficiencies. Therefore, the temperature in the column should be kept

homogeneous. The small heat capacity of micro-HPLC columns also facilitates application of temperature programming in LC.

Another advantage of micro-HPLC is the possibility of direct coupling with exotic detectors such as a mass spectrometer. The lower the flow rate of the mobile phase, the easier direct coupling with MS becomes.

### 3. Instrumentation

#### 3.1. Pumping system

In order to achieve the same retention time independent of the column diameter the flow rate must be adjusted so that the linear velocity is kept constant. Micro-HPLC therefore requires a pump that provides flow rates between 1 to 10  $\mu\text{l}/\text{min}$ . High-pressure micro-pumps are now commercially available. A microfeeder (Azumadenki Kogyo, Tokyo, Japan) equipped with a gas-tight syringe is the prototype pump that has been employed in our laboratory. It can withstand an approximately 70  $\text{kgf}/\text{cm}^2$ , and the flow rates of less than 1  $\mu\text{l}/\text{min}$  can be generated with good precision. Several milliliters of solvent is enough for one-day operation including the volume required to rinse the pump. When higher-pressure operations are required, commercially available high-pressure pumps should be used.

#### 3.2. Injection system

##### *Valve injection*

The injection volume should be carefully selected in consideration of the column dimensions. Roughly speaking, the injection volume should be less than one-hundredth of the column volume. For example, when a microcolumn with a 0.25-mm ID and 100-mm length is employed, the injection volume should be reduced to approximately 0.02  $\mu\text{l}$ .<sup>10)</sup> Such a small volume can now be loaded with good reproducibility by using a commercially available injector, e.g., an ML-422 (or 425) microvalve injector (JASCO, Tokyo, Japan). The injection volume of this injector can be altered by changing the dimension of the hole in the rotor disk. Several disks with different volume are provided for this injector. Rheodyne 7520 (Cotati, CA, USA) and EYELA 5001 (Tokyo, Japan) valve injectors are based on the same operation principle as the ML-422 injector. The operating principle of such injectors is schematically shown in Fig. 1.

Fig. 2 demonstrates the good reproducibility of valve injection.<sup>11)</sup> It is remarkable that the 0.6% relative standard deviation for the peak heights of successive 15 measurements was obtained even though the injection volume is as small as 0.02  $\mu\text{l}$ .

The connecting tubing between the column and the injector also plays an important role to obtain satisfactory results. Narrow-bore tubing with around 50- to 70- $\mu\text{m}$  ID should be employed as the connecting tubing in order to reduce the extracolumn band broadening.

##### *Precolumn concentration*

Increased mass sensitivity due to miniaturization of the columns is useful in trace analysis and is especially favourable in the analysis of precious samples. However, valve injection spoils most of the samples and valve injection is not preferred in the analysis of valuable samples, such as components present in blood serum. The precolumn concentration method is an effective solution to this problem. In this method, the adequate volume of sample solution is passed through the precolumn prior to the chromatographic run and all the concentrated solutes in the precolumn are then subjected to chromatographic separation. Solutes of interest

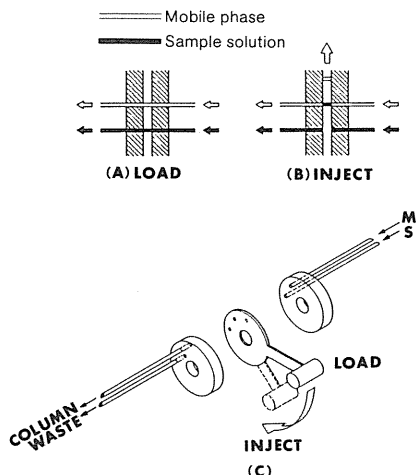


Fig. 1 Operating principle of the microvalve injector employed in this work.<sup>11)</sup>  
 (A) and (B): Operating principle. (C): Injection of sample solution into the column by changing the disc position from LOAD to INJECT. M: mobile phase. S: sample.

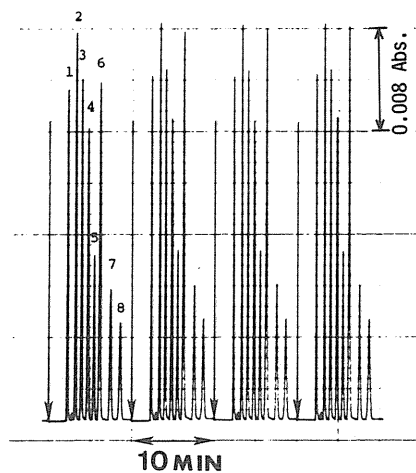


Fig. 2 Reproducibility of the peak height.<sup>11)</sup>  
 Column:  $100 \times 0.25$  mm ID packed with  $5\text{-}\mu\text{m}$  ODS. Mobile phase: acetonitrile-water (70:30). Flow rate:  $3\ \mu\text{l}/\text{min}$ . Wavelength of UV detection: 254 nm.  
 Samples: 1 = benzene; 2 = naphthalene; 3 = biphenyl; 4 = fluorene; 5 = phenanthrene; 6 = anthracene; 7 = fluoranthene; 8 = pyrene.

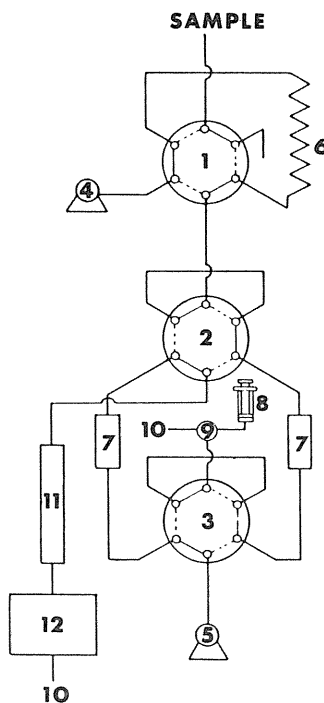


Fig. 3 Diagram of a precolumn concentration system.<sup>12)</sup>  
 1 = switching valve (Rheodyne 7000); 2 = switching valve (Valco N6W); 3 = switching valve (Rheodyne 7000); 4 = pump (JASCO FAMILIC-300S); 5 = pump (LKB 2150); 6 = sample loop; 7 = enrichment columns; 8 = gas-tight syringe for the measurement of the sample volume; 9 = three-way stopcock; 10 = drain; 11 = separation column; 12 = UV detector.

can be effectively concentrated in the enrichment column by selecting the proper packing material and altering the property of the matrix solution. In addition, the precolumn concentration method improves the concentration sensitivity of micro-HPLC. When the concentration of a solute is 1 ppb, 1 ng of the solute is subjected to the separation if 1 ml of the sample solution is passed through the precolumn and recovery is perfect.

An on-line precolumn concentration system can be constructed by using commercially available switching valves.<sup>12)</sup> Fig. 3 shows an on-line precolumn concentration system consisting of two pumps, three switching valves, two enrichment columns, a separation column, and a detector. The system with two enrichment columns allows concentration of the sample solution in one enrichment column, while the other enrichment column is used for analysis. In order to minimize sample band broadening in the parts between the separation column and the enrichment columns, narrow-bore tubing should be employed as the connecting tubing to the N6W switching valve (Valco, Houston, TX, USA). The N6W switching valve is originally developed for capillary GC and it has tolerable dead volume for micro-HPLC.

### 3.3. Column preparation

The packing procedure for micro-HPLC columns is basically the same as that for conventional HPLC columns except for the dimension of the packer. Various packing techniques have been reported for HPLC, among which a slurry packing technique is one of the recommended method for the preparation of the micro-HPLC columns.

Various types of column tube materials such as PTFE, stainless-steel, glass, fused-silica or glass-lined stainless-steel tubing have been utilized in micro-HPLC. Among these the fused-silica and glass-lined stainless-steel columns give higher efficiencies, due to their smooth and inert surface.<sup>10),13)</sup>

Fused-silica tubing is flexible, which is convenient for handling long columns. Polyimide ferrules that permit high-pressure operation are commercially available for fused-silica tubing.

Glass-lined stainless-steel tubing with different inner diameters is also commercially available. Glass-lined stainless-steel tubing with a 1/16 inch OD is capable of connecting the column with commercially available unions, facilitating the preparation and operation of the column under high pressure.

In addition, micro-HPLC columns can be manually prepared by using a gas-tight syringe when the column length is shorter than around 20 cm.

### 3.4. Detection system

Various types of detectors have been employed in HPLC. Among them the UV/visible, fluorescence, electrochemical detectors and refractometers are the most common. In order to utilize these detectors in micro-HPLC, their flow cells must be modified. Basically the flow cell volume must be reduced so that the band broadening in the detection part may not deteriorate the column efficiency.

The flow cell used in the optical detector can be divided into two types according to its structure: the parallel-flow cell and the cross-flow cell, as shown in Fig. 4. The former is capable of producing higher sensitivity, but preparation of such a microflow cell is difficult. The latter uses a cylindrical quartz as the flow cell, and the dead volume of the connection between the separation column and the flow cell can be minimized. In the special case a portion of the separation column itself can be employed as the flow cell, i.e., on-column detection.

Voltammetric detectors have a real advantage for microcolumns because the low flow rates actually favour electrode efficiency and, even when the cell volume is reduced, sensitivity does not have to be sacrificed. The miniaturized voltammetric detectors with a single

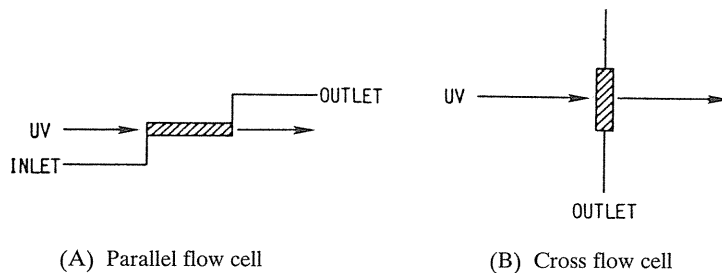


Fig. 4 Structures of flow cells for optical detectors.

working electrode can be divided into two types: thin-layer cells and tubular cells. In the thin-layer cell, the cell cavity is constructed of two fluorocarbon resin blocks separated by a 20–45- $\mu\text{m}$  thick and 0.5–2-mm wide PTFE sheet.<sup>14)</sup> A working electrode is made with glassy carbon disks of 3 mm diameter and contained in one of the blocks. The silver-silver chloride reference electrode is held in a cylindrical hole in the other block. A stainless-steel tube serves both as the counter electrode and the exit line. The cell volume of such cells is about 0.06–0.1  $\mu\text{l}$ .

For open-tubular capillary LC Knecht *et al*<sup>15)</sup> developed a tubular type cell with a single graphite fiber electrode. The working electrode is constructed from a single carbon fiber with a 9- $\mu\text{m}$  diameter and about 0.7-mm length, which can be inserted with a micropositioner into the outlet end of the capillary column. A glass vessel is constructed to surround the fiber with 0.1 M potassium chloride electrolyte solution and to furnish the silver-silver chloride electrode.

Miniaturized voltammetric detectors with two working electrodes were also designed for micro-HPLC.<sup>16)</sup> Two types of configuration, serial and parallel, of the two working electrodes with respect to the flow axis. In series configuration, the working electrodes are positioned along the flow stream on one side of the channel. In parallel configuration, the working electrodes are placed opposite one another on both sides of the channel. The series dual voltammetric detector is analogous to the fluorometric detector, and the product of the electrode reaction at the upstream working electrode is detected at the downstream working electrode. On the other hand, the parallel dual voltammetric detector is analogous to the photomultiplier tube, and the product of the electrode reaction at one working electrode can diffuse to the opposite working electrode where starting material may be created.

Use of a mass spectrometer as the detector for HPLC has been investigated because the mass spectrum gives one of the most useful information for the identification of the analyte. Although some types of HPLC/MS are now already commercially available, HPLC/MS is not yet sufficiently matured. The authors have also examined direct coupling of micro-HPLC and fast atom bombardment MS (FABMS),<sup>17)</sup> which will be discussed in detail later.

Multichannel UV-visible detectors are capable of recording a series of absorption spectra in a single chromatographic run. The multichannel detection has many advantages over conventional single-wavelength detection: improved identification; ability to check the purity of chromatographic peaks; and rapid selection of an optimal wavelength. A multichannel, photodiode array UV/visible detector can also be applied in micro-HPLC by decreasing the number of optical parts, such as lenses and mirrors, and by reducing the distance between

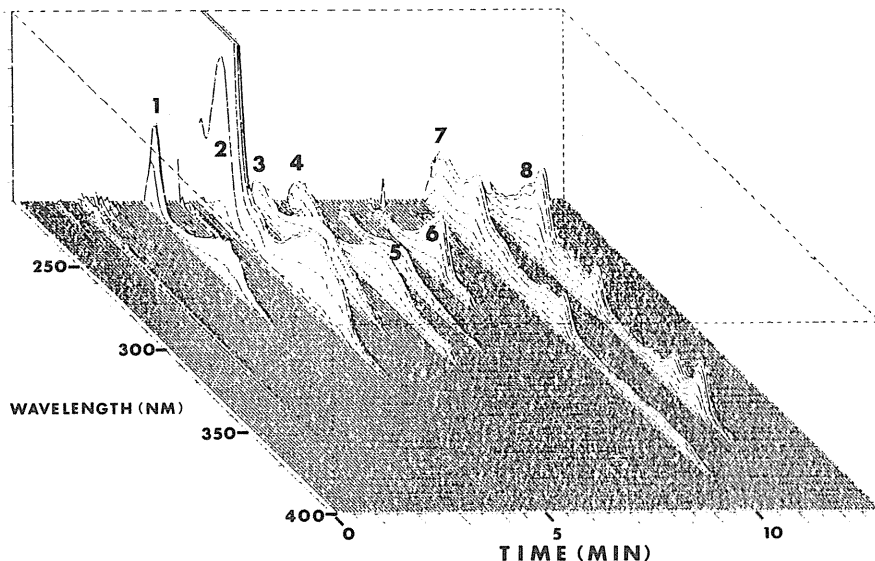


Fig. 5 A three-dimensional chromatogram of polynuclear aromatic hydrocarbons.<sup>18)</sup> Column:  $140 \times 0.34$  mm ID packed with  $5\text{-}\mu\text{l}/\text{min}$ . Mobile phase: acetonitrile-water (65:35). Flow rate:  $5.6\ \mu\text{l}/\text{min}$ . Samples: 1 = benzene; 2 = naphthalene; 3 = biphenyl; 4 = fluorene; 5 = phenanthrene; 6 = anthracene; 7 = fluoranthene; 8 = pyrene.

the light source and the flow cell and between the flow cell and the grating.<sup>18)</sup> A three-dimensional chromatogram of polynuclear aromatic hydrocarbons is shown in Fig. 5.<sup>18)</sup>

## 4. Application

### 4.1. Catecholamines and their metabolites

Catecholamines play an important role in the central nervous system and in neurological diseases. Consequently, their separation and determination have received considerable attention. Numerous techniques have been developed for the quantitation of catecholamines. The approaches include fluorescence detection, radioenzymatic methods, HPLC coupled with fluorometric detection and HPLC coupled with electrochemical detection. Among them, HPLC coupled with electrochemical detection provides a sensitive and selective analytical method.

Fig. 6 shows typical chromatograms of catecholamines in human serum from healthy individuals obtained using the precolumn concentration method with an alumina enrichment column.<sup>19)</sup> A micro-HPLC system with the parallel dual voltammetric detector was used. Of particular interest in parts A are the peaks appearing as the shoulder of NA in Fig. 6b and the background of AD in Fig. 6a, respectively. By recording the cathodic current, the interferences from the compounds responsible for these peaks could be removed, as shown in parts B, on the basis of their electrochemical irreversibility. The parallel dual voltammetric



detector provides an enhancement in sensitivity by recycling oxidation and re-reduction between the anode and cathode at slow flow rates of the mobile phase.

Fig. 7 shows the chromatograms of catecholamine metabolites in urine from two healthy individuals, separated on a microcolumn packed with 5- $\mu\text{m}$  ODS and using the series dual voltammetric detector.<sup>20</sup> The urine sample was acidified, spiked with hydroquinone as the internal standard, and extracted with ethyl acetate. The organic solvent was evaporated to dryness with a stream of nitrogen gas, the residue being dissolved with the mobile phase. The extracted urine (0.3  $\mu\text{l}$ ) was injected. Parts A and B in Fig. 7 are the anodic chromatograms obtained with the upstream working electrode and the cathodic chromatograms obtained with the downstream working electrode, respectively. The peaks appearing as the background of homovanillic acid are of particular interest in part A. By recording the re-reduction current, the interferences from the compounds responsible for these peaks could be removed, as shown in part B, on the basis of their electrochemical irreversibility.

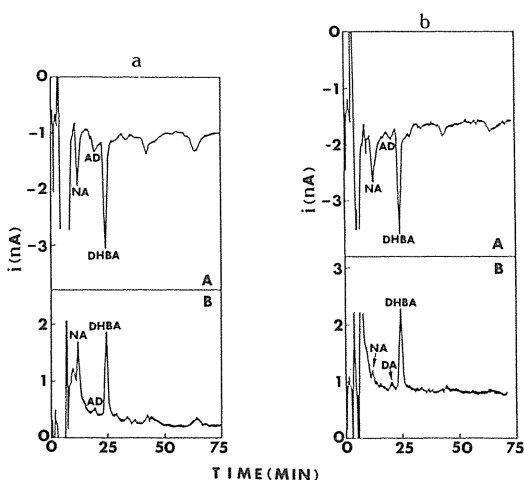


Fig. 6 Typical chromatograms of catecholamines in human serum from healthy individuals by internal standard addition.<sup>19</sup> (A) Anodic response, (B) cathodic response. Column: 150  $\times$  0.5 mm ID packed with 10- $\mu\text{m}$  ODS. Enrichment column: 20  $\times$  0.5 mm ID packed with 30- $\mu\text{m}$  alumina. Mobile phase: B-R buffer (pH = 1.8) containing 2 mM sodium 1-heptanesulphonate, 0.1 mM EDTA and 50 mM sodium perchlorate. Flow rate: 8.3  $\mu\text{l}/\text{min}$ . Applied potentials (versus Ag/AgCl): 0.06 and 0.20 V. Sample: 200  $\mu\text{l}$  of human serum spiked with 100 pg of DHBA. Peak identification: noradrenaline (NA); adrenaline (AD); 3,4-dihydroxybenzylamine (DHBA).

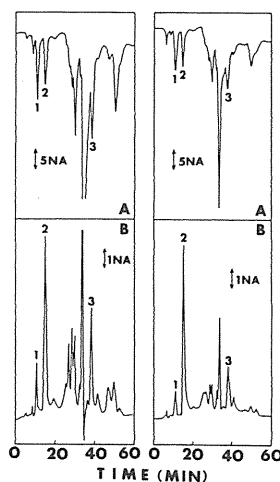


Fig. 7 Selective detection of catecholamine metabolites in urine from two healthy individuals (a, b) with a series dual voltammetric detector.<sup>20</sup> (A) Anodic response, (B) cathodic response. Applied potentials (versus Ag/AgCl): anode, +0.90 V; cathode, -0.05 V. Column: 154  $\times$  0.5 mm ID packed with 5- $\mu\text{m}$  ODS. Mobile phase: methanol-0.1 M phosphate buffer (pH 3.6) containing 0.1 mM EDTA (methanol concentration was stepwise increased from 5% to 25% in 23 min). Flow rate: 5.6  $\mu\text{l}/\text{min}$ . Peaks: 1 = vanillylmandelic acid; 2 = hydroquinone (int. std.); 3 = homovanillic acid.

#### 4.2. Bile acids

Analysis of bile acids in serum is required for diagnostic purposes because the abnormal presence of bile acids reflects a functional disorder of the liver. The increased mass sensitivity of micro-HPLC is significant in the analysis of biological samples.

HPLC analysis of bile acids with 3 $\alpha$ -hydroxysteroid dehydrogenase (3 $\alpha$ -HSD) post column derivatization<sup>21)</sup> seems promising with respect to resolution, sensitivity, and quantitation, as compared with GC, GC/MS, thin-layer chromatography and HPLC using ultraviolet and refractive index detectors. In the method using a post-column enzyme reaction, the 3 $\alpha$ -hydroxy group in each bile acid is oxidized to a keto group, while simultaneously  $\beta$ -nicotinamide adenine dinucleotide (NAD) is reduced to NADH, which is subjected to fluorescence detection.

Fig. 8 demonstrates the separation of an artificial mixture of 15 bile acids on an ODS column.<sup>22)</sup> The bile acids (approximately 20 ng each) are detected by a fluorescence detector and the mass sensitivity is increased by a factor of 50, as compared to conventional HPLC. The detection limit (signal to noise ratio: 2) is 0.13–0.28 pmole.

Fig. 9 illustrates the separation of bile acids in 0.1 ml serum of a patient with alcoholic cirrhosis and of a healthy volunteer.<sup>22)</sup> The serum was diluted ten times in 10-mM phosphate solution (pH = 7–8). One ml of the phosphate solution of the serum was drawn into a gas-tight syringe and forced into an enrichment column. Bile acids could be determined by monitoring NADH at 365 nm for excitation and at 470 nm for emission. The difference in the amounts of bile acids between two chromatograms is significant.

#### 4.3. Amino acids

Liquid chromatographic analysis of amino acids have been investigated by many researchers in food chemistry, biochemistry and clinical chemistry. Sequence analysis of amino acids of proteins or peptides is the most well-known project in this field. Since most amino acids do not possess intrinsic fluorescing nor UV-absorbing moieties in their molecules, pre-column or postcolumn derivatization processes have been involved in the trace analysis of amino acids by HPLC, and consequently various derivatization methods and reagents have been developed for this purpose.

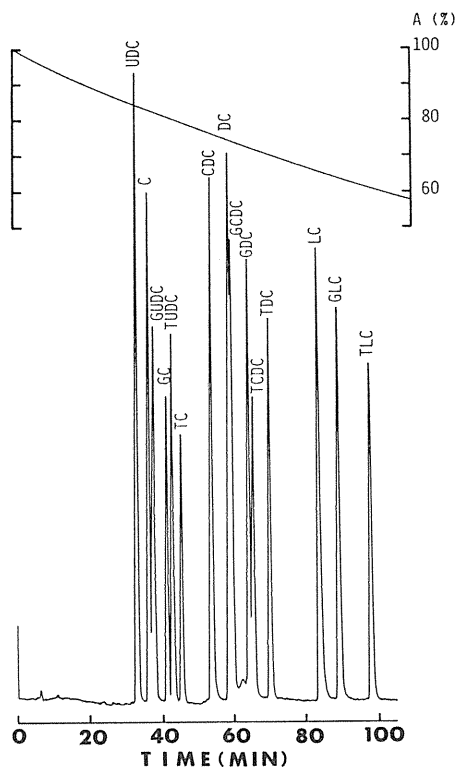


Fig. 8 Separation of an artificial mixture of bile acids.<sup>22)</sup> Separation column: 200  $\times$  0.26 mm ID packed with 5- $\mu$ m ODS. Post-column: 3 $\alpha$ -HSD, 20  $\times$  0.34 mm ID. Mobile phase: (A) acetonitrile/60 mM phosphate solution (pH: 9.8)/60 mM phosphate solution (pH: 8.9) containing 18 mM NAD (20/70/10); (B) acetonitrile/60 mM phosphate solution (pH: 9.5)/60 mM phosphate solution (pH: 8.9) containing 18 mM NAD (60/30/10), gradient profile is indicated. Flow rate: 2.1  $\mu$ l/min. Wavelengths of detection: Ex. 365 nm; Em. 470 nm.

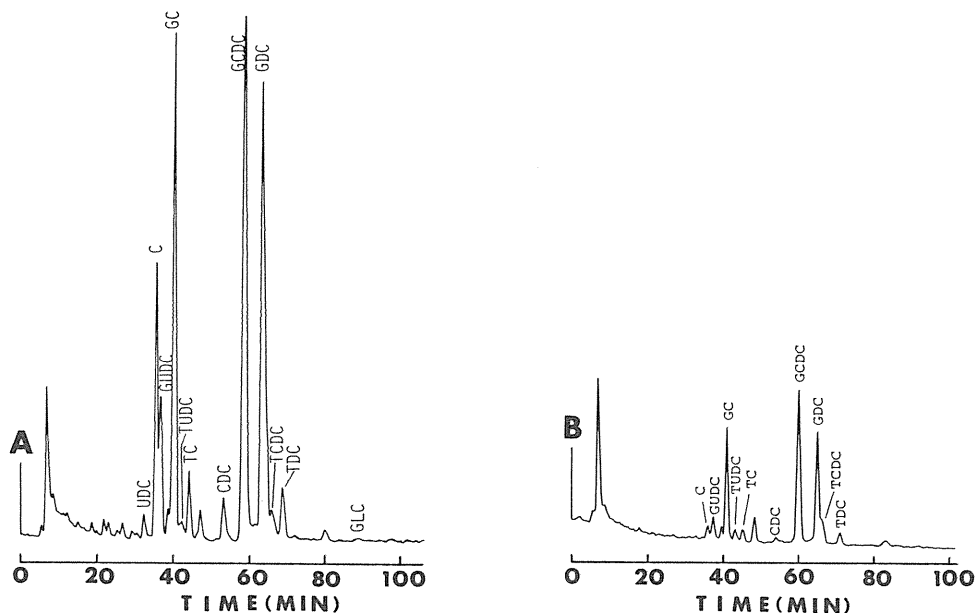


Fig. 9 Separation of bile acids in the serum of a patient with alcoholic cirrhosis (A) and of a healthy volunteer (B).<sup>22)</sup> Operating conditions as in Fig. 8, except for the following. Enrichment column: Develosil ODS-15/30 (15-30  $\mu\text{m}$ ),  $10 \times 0.2$  mm ID. Sample: 0.1 ml of serum from a patient with alcoholic cirrhosis (A) and from a healthy volunteer (B).

Derivatization with 5-dimethylaminonaphthalenesulphonyl (Dns or Dansyl) chloride is known as one of the very sensitive HPLC methods for amino-acid analysis. Fig. 10 demonstrates the gradient elution of separation of an artificial mixture of dansyl amino acids and those in sake.<sup>23)</sup> Dansyl derivatization of amino acids in sake was carried out at  $38^\circ\text{C}$  for 1–2 hr after adjusting the pH of the sample solution to 9.7. The high concentration of the amino acids in this sample permitted injection of a small sample volume (0.02  $\mu\text{l}$ ) with a valve injector. The injected amounts corresponded to 11 nl of sake. The mass detection limit (signal-to-noise ratio: 2) was approximately 0.1 pmol.

Resolution of optical isomers of amino acids is another important project. The resolution of enantiomers of amino acids have been carried out by using a chiral stationary phase, incorporating a chirality-recognizing reagent in the mobile phase or derivatization into the corresponding diastereoisomers. Various types of the chiral stationary phases have been developed for the separation of amino acid enantiomers. On the other hand, optical resolution by the second approach relies on chiral recognition by ligand exchange, ion-pair formation or complexation between the additive and the analyte.

It is well-known that cyclodextrins show high stereoselectivity. They form inclusion complexes with a variety of molecules and ions. There are three cyclodextrins of different sizes available commercially, which differ in the number of glucose units in the ring. The cavity size of  $\beta$ -cyclodextrin is suitable to form inclusion complexes with compounds that have a naphthalene ring.

Enantiomers of dansyl amino acids have been successfully separated on a  $\beta$ -cyclodextrin-bonded phase with a mobile phase of methanol and water,<sup>24)</sup> where the L isomer of

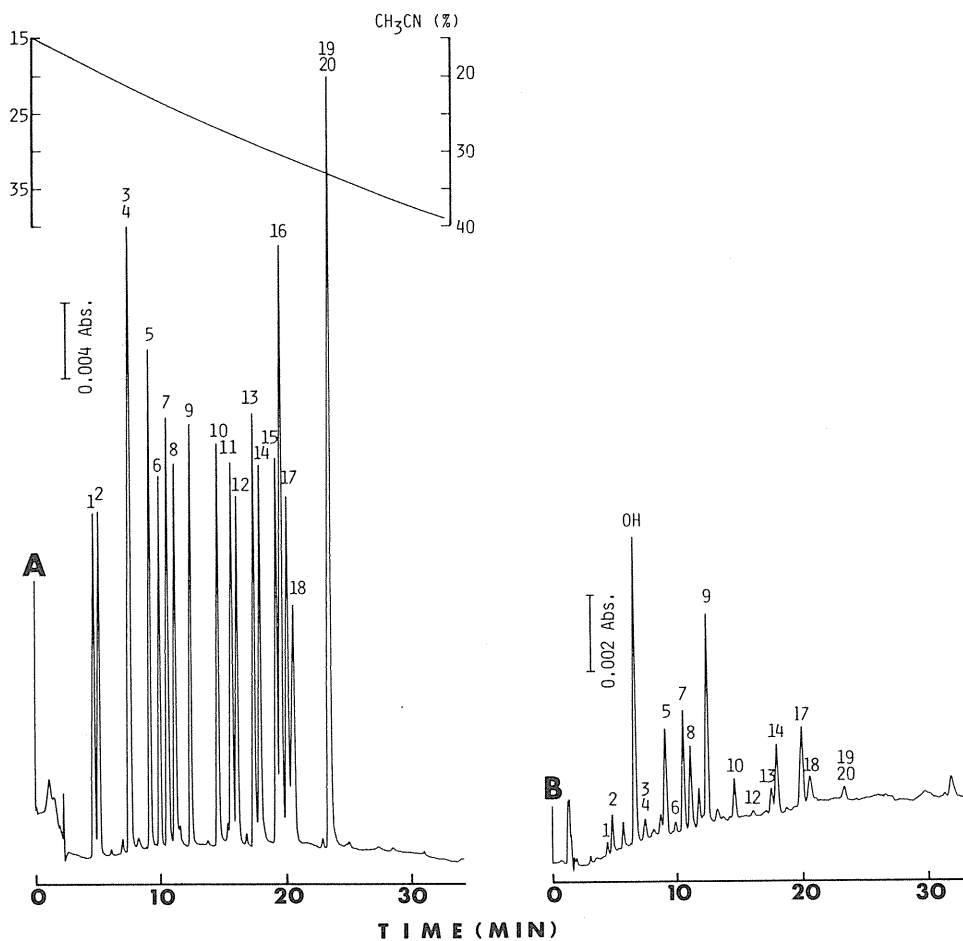


Fig. 10 Separation of an artificial mixture of dansyl amino acids (A) and those in sake (B)<sup>23</sup>. Column:  $100 \times 0.34$  mm ID packed with 3- $\mu$  ODS. Mobile phase: acetonitrile/0.13 M ammonium acetate with the gradient profile as indicated. Flow rate: 4.2  $\mu$ l/min. Samples: 1=Asp; 2=Glu; 3=Hyp; 4=Asn; 5=Ser; 6=Thr; 7=Gly; 8=Ala; 9=Pro; 10=Val; 11=Nval; 12=Met; 13=Ile; 14=Leu; 15=Nleu; 16=Trp; 17=Phe; 18= $\text{NH}_2$ ; 19=di-Cys; 20=Cys; OH=dansylic acid. Sample amounts: (A) 40 pmol each; (B) 11 nl of sake. Wavelength of UV detection: 222 nm.

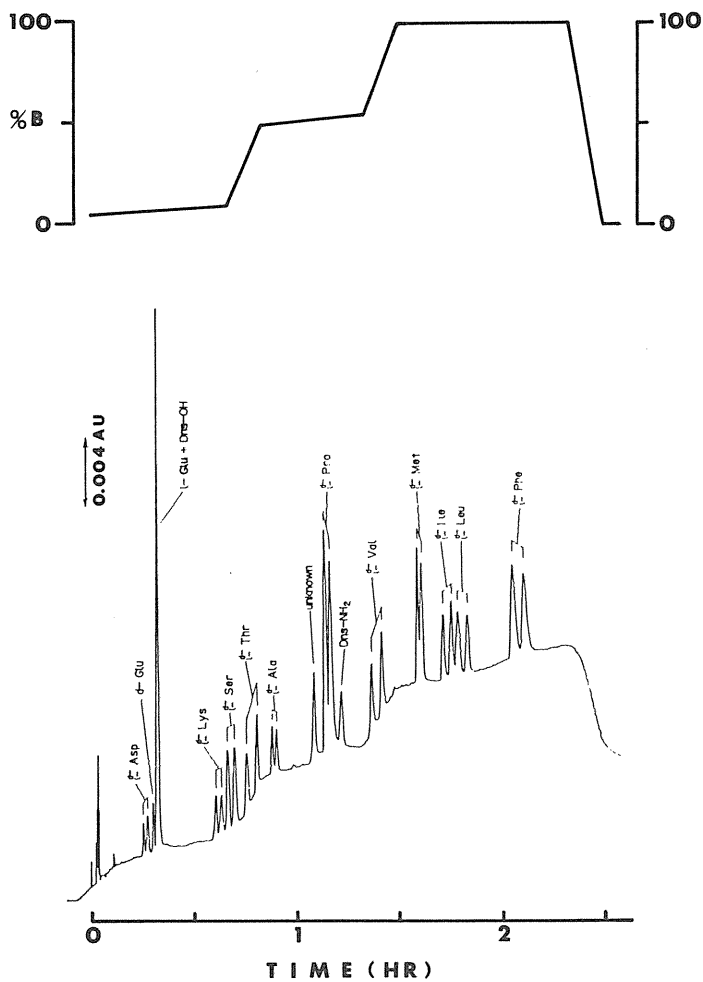


Fig. 11 Gradient separation of racemic dansyl amino acids.<sup>25)</sup> Column:  $144 \times 0.3$  mm ID packed with  $3\text{-}\mu\text{m}$  ODS. Mobile phase: (A) acetonitrile-phosphate buffer (10:90) containing 12.5 mM  $\beta$ -cyclodextrin (pH 6.4); (B) acetonitrile-phosphate buffer (20:80) containing 12.5 mM  $\beta$ -cyclodextrin (pH 6.4) with the gradient profile as indicated. Flow rate:  $5.0 \mu\text{l}/\text{min}$ . Sample: 20 pmol each.

a dansyl amino acid elutes before its D isomer. This indicates that the inclusion complex with the D isomer is more stable than that with the L isomer. In the case of the separation with a mobile phase including  $\beta$ -cyclodextrin, the D isomer can be expected to elute before its L isomer because, as the stability of the isomer increases, the isomer is less retained on the stationary phase.

Fig. 11 demonstrates the gradient separation of twelve pairs of dansyl amino acids using a mobile phase including  $\beta$ -cyclodextrin and a non-chiral stationary phase, ODS.<sup>25)</sup>

Precolumn derivatization into the diastereoisomers allows indirect separation of enantiomers. The diastereoisomers can be separated on a non-chiral column. Derivatization of amino acids with o-phthalaldehyde (OPA) and a chiral thiol has been one of the successful methods for the separation of many pairs of the amino acid enantiomers<sup>26)</sup> in a single chromatographic run. With this method fourteen pairs of amino acid enantiomers could be separated by micro HPLC after precolumn derivatization with OPA and N-acetyl-L-cysteine.<sup>27)</sup>

#### 4.4. Proteins

HPLC has been of great use for the analysis of biological samples. Proteins have been separated by reversed-phase chromatography, ion-exchange chromatography, size-exclusion chromatography (SEC), chromatofocusing, etc. Since protein samples are usually complex mixtures, it is preferable to use a high resolution technique for their analysis. In addition, the protein samples are sometimes only available in very small amounts, so that the miniaturized techniques are generally appreciated in biological analyses. These requirements are satisfied in micro-HPLC: preparation of high-efficiency columns producing 200,000 plate numbers or more is possible.<sup>28)</sup> Applications of the microcolumn techniques to the analysis of proteins by SEC and chromatofocusing are described in this section.

##### *Size-exclusion chromatography*

SEC gives us information regarding the molecular size of peaks, which is an added advantage of SEC. It is for this reason that SEC has been employed for the separation of proteins, even though it has lower peak capacity compared with that of other chromatographic separation modes. The peak capacity in SEC can be improved by increasing column length, i.e., producing larger theoretical plate numbers.<sup>29)</sup> The multiple detection system with one detector has been developed to facilitate the use of long columns.<sup>30)</sup> The chromatograms obtained with the multiple detection system is shown in Fig. 12.<sup>30)</sup>

##### *Chromatofocusing*

Chromatofocusing is a method for separating amphoteric substances through differences in their isoelectric points, so that it is useful for the analysis of proteins and peptides. In this method so-called internal pH gradient is used, which is produced on the ion exchanger in the column using a carrier-ampholytes buffer solution; not by mixing two solutions as in the ordinary gradient technique. Proteins are adsorbed on the base of their pI(s) and as the result separated to components.

High-resolution chromatofocusing is demonstrated in Fig. 13 using a slurry-packed capillary column.<sup>31)</sup> The longer column gave better resolution. Prior to the chromatographic run, the column was conditioned with 20-mM glycine solution, pH of which was adjusted to pH 9.7 with aqueous ammonia solution. A 0.2% Ampholine solution of pH 7.6 was then pumped into the separation column. In addition, it was found that the first analysis gave the best resolution. The regeneration of the used column by washing with various kinds of aqueous solutions and organic solvents was not successful. Therefore, when better resolution is required, microcolumns should be considered as semi-disposable one taking advantage of their low cost.<sup>32)</sup>

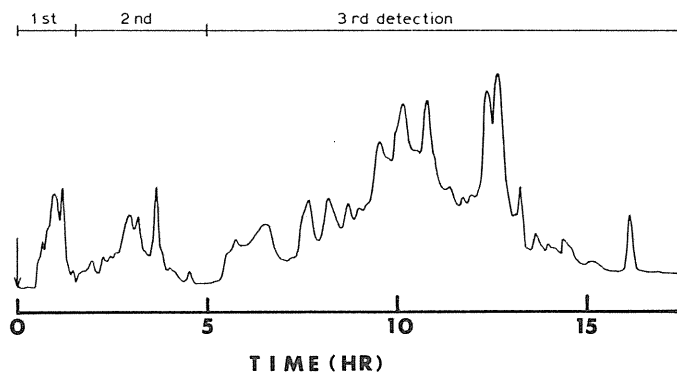


Fig. 12 Application of the multiple detection system to the separation of urease.<sup>30)</sup> Column: 0.26 mm ID packed with 10- $\mu$ m TSKgel G3000SW (TOSOH). Column lengths: 1st, 1 m; 2nd, 3.5 m; 3rd, 9.5 m. Eluent: 0.2 M phosphate buffer. Wavelength of UV detection: 220 nm.

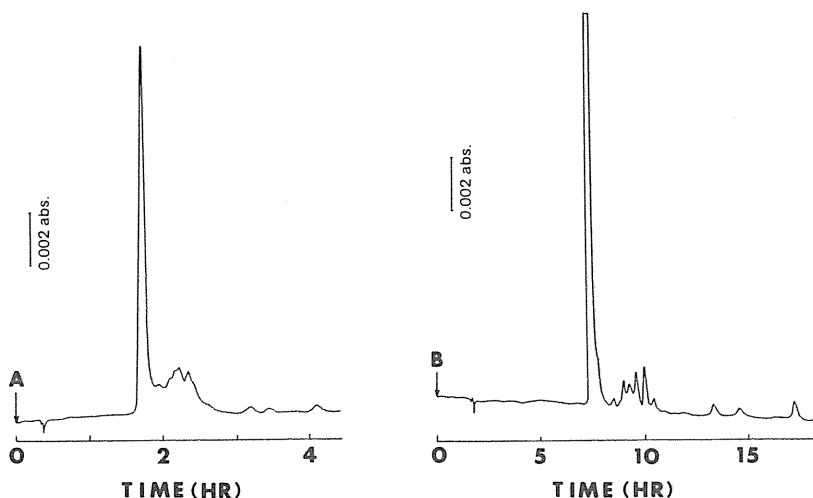


Fig. 13 Separation of sperm whale myoglobin by chromatofocusing.<sup>31)</sup> Columns: (A) 0.45 m  $\times$  0.25 mm ID packed with 10- $\mu$ m TSKgel DEAE-5PW (TOSOH); (B) 2.2 m  $\times$  0.25 mm ID packed with the same material as in (A). Eluent: 0.2% Ampholine solution of pH 7.6. Wavelength of detection: 409 nm.

#### 4.5. Industrial chemicals

HPLC has widely been applied to characterization, molecular-weight determination and trace analysis of industrial chemicals including polymers, additives in polymers, detergents, pesticides, herbicides, petroleum, lipids, etc. This section introduces application of micro-HPLC to epoxy resin oligomers and antioxidants in gasoline.

The byproducts of the epoxy resin production are compounds having functional groups other than epoxide groups, either as end groups or as side chains. As these byproducts affect

the property of epoxy resins, their characterization is of practical importance. Size-exclusion chromatography, reversed-phase liquid chromatography, and field-desorption mass spectrometry have been utilized to characterize epoxy resin oligomers. Separation of the epoxy resin oligomers by micro-HPLC was investigated in the reversed-phase and size-exclusion modes.

Micro-HPLC facilitates the use of long columns providing large theoretical plate numbers. Fig. 14 shows the separation of epoxy resin, Epikote 1001, in the size-exclusion and reversed-phase modes.<sup>33),34)</sup> In the former case a 2-m column packed with 5- $\mu\text{m}$  polystyrene gel is used, while in the latter case a 0.5-m column packed with 5- $\mu\text{m}$  ODS is used. Reversed-phase liquid chromatography generally results in a much better resolution of the oligomer than size-exclusion chromatography.

The micro precolumn concentration method was applied to the analysis of antioxidants in gasoline.<sup>35),36)</sup> Antioxidants such as *p*-phenylenediamines could be concentrated on alumina or silica gel enrichment columns followed by separation in the reversed-phase mode. A multichannel photodiode array detector is suitable for the measurement. Fig. 15 shows the

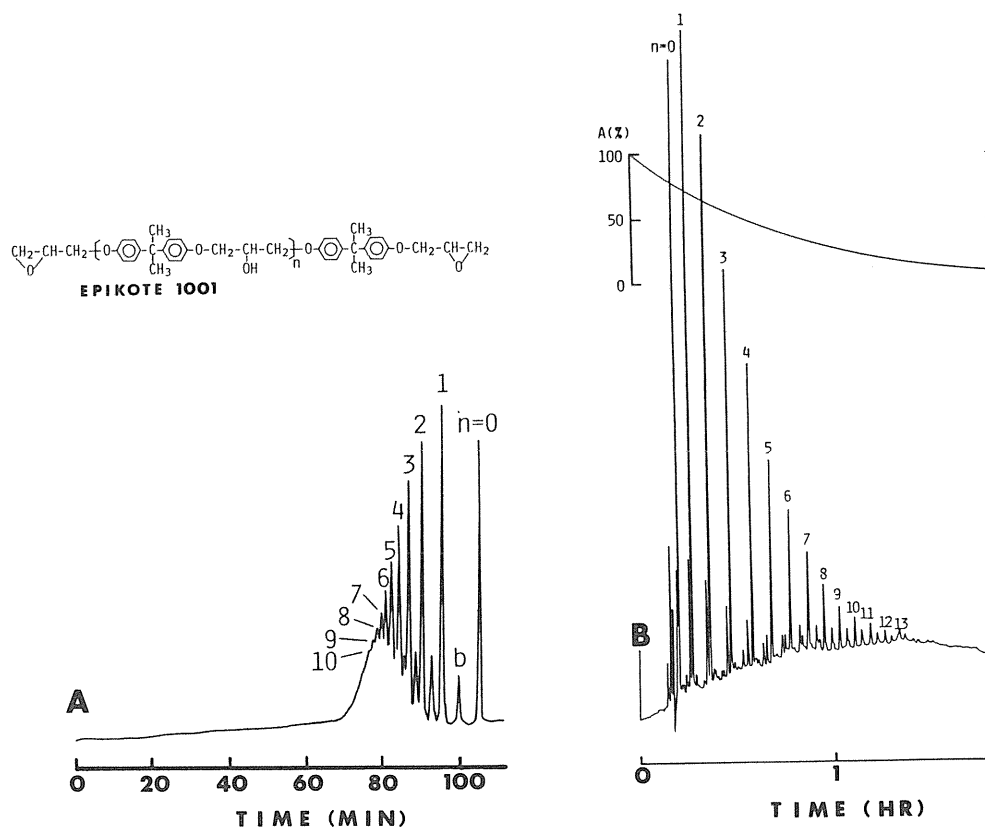


Fig. 14 Separation of Epikote 1001 in the size-exclusion (A) and reversed-phase mode (B).<sup>33),34)</sup> Columns: (A) 2 m  $\times$  0.35 mm ID packed with 5- $\mu\text{m}$  polystyrene gel having the exclusion limit of  $2 \times 10^4$  molecular weight; (B) 0.5 m  $\times$  0.35 mm ID packed with 5- $\mu\text{m}$  ODS. Mobile phases: (A) tetrahydrofuran; (B) A = acetonitrile/water (85:15); B = acetonitrile/tetrahydrofuran (90:10), gradient profile as indicated. Flow rates: (A) 1.0  $\mu\text{l}/\text{min}$ ; (B) 1.4  $\mu\text{l}/\text{min}$ . Wavelength of UV detection: (A) 280 nm.; (B) 225 nm.



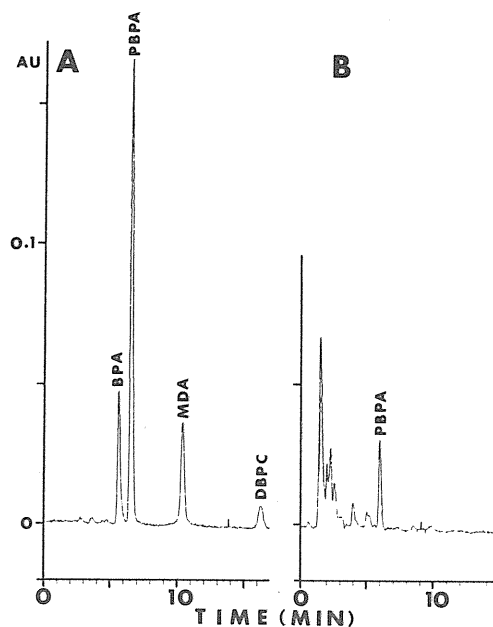


Fig. 15 Separation of antioxidants and a metal deactivator.<sup>35)</sup> Column:  $150 \times 0.34$  mm ID packed with  $5\text{-}\mu\text{m}$  ODS. Enrichment column:  $10 \times 0.2$  mm ID packed with  $10\text{-}\mu\text{m}$  silica gel. Mobile phase: acetonitrile/water/n-hexylamine (65:35:1). Flow rate:  $5.6 \mu\text{l}/\text{min}$ . Samples: (A) standard; (B)  $1 \mu\text{l}$  gasoline. Peaks: BPA = *N,N'*-di-sec.-butyl-*p*-phenylenediamine; PBPA = *N*-phenyl-*N'*-sec.-butyl-*p*-phenylenediamine; MDA = *N,N'*-disalicylidene-1,2-propanediamine; DBPC = 2,6-di-tert.-butyl-*p*-cresol. Wavelength of UV detection: 290 nm.

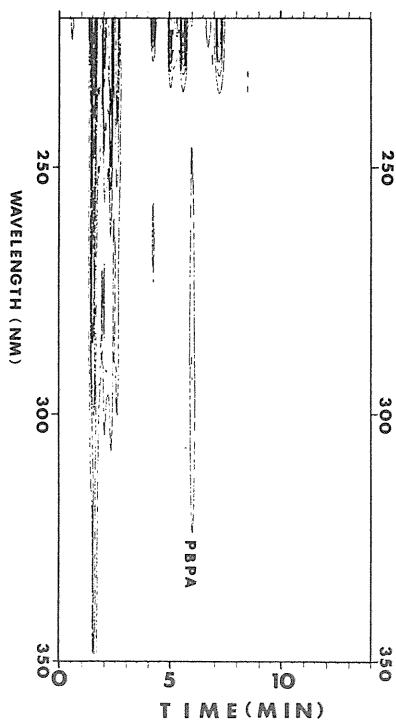


Fig. 16 A contour plot of the gasoline sample.<sup>36)</sup> Operating conditions as in Fig. 15. PBPA = *N*-phenyl-*N'*-sec.-butyl-*p*-phenylenediamine.

separation of a mixture of various diamines and the components of gasoline.<sup>36)</sup> The gasoline sample was diluted 300 times with hexane and  $300 \mu\text{l}$  of the diluted sample was passed through a silica gel enrichment column. Thus the chromatogram corresponds to  $1 \mu\text{l}$  gasoline.

Fig. 16 illustrates a contour plot of the gasoline sample.<sup>36)</sup> Such a plot is useful for selecting the optimal conditions for the determination by single-wavelength detection.

## 5. Microcolumn-based detection

New detection methods for micro-HPLC are described in this chapter, involving fast-atom bombardment mass spectrometric (FABMS), on-column fluorometric and indirect photometric detection. These new detection methods are attributed to attractive features

of micro-HPLC, e.g., small column diameters, low flow rates of the mobile phase, and low heat capacity of the separation column.

### 5.1. Direct combination with FABMS

Direct coupling of HPLC and MS was expected to provide a versatile analytical method but many more difficulties have been encountered in the combination of these two mismatched analytical tools than in GC/MS. Nevertheless, many challenging investigations have been devoted to development of new interfacing and improvement of the mismatch between HPLC and MS.

In on-line HPLC/MS, effluent from the separation column continuously enters into the mass spectrometer source chamber via various means such as direct liquid introduction, thermospray, moving belt methods, etc., to be ionized before being transferred to the mass analyzer. Various types of ionization techniques, involving solid-phase, liquid-phase and gas-phase ionization, have been examined; recent developments include thermospray, atmospheric-pressure ionization, MAGIC EI (monodisperse aerosol generator for introduction of liquid chromatographic effluent, electron impact), fast-atom bombardment (FAB) ionization, etc.

FABMS is an excellent technique for the analysis of thermally unstable and/or involatile polar compounds with high molecular weights,<sup>37),38)</sup> and as such has played an important role in biopolymer structure elucidation. For the measurement of FAB mass spectra, the analyte dispersed in an adequate matrix such as glycerol is placed on a target, which is bombarded by an argon or xenon beam. FAB is a soft ionization technique, and it generally provides quasi-molecular ions as well as fragment ions, which are useful for identifying the analytes. It should be noted that analytes must be pure for identification by MS. In order to exempt time-consuming, troublesome tasks for the purification process, combination with chromatography or tandem MS are attractive options.

In combining HPLC and FABMS, effluent from the separation column must be transferred onto the target in the ion source and the analyte must be dispersed in a suitable matrix. Mobile phase components interfere with mass spectra and degrade the vacuum. Therefore, the less the introduction of the mobile phase, the better the result obtained.

Two approaches for HPLC/FABMS have been investigated, involving a moving belt method<sup>39)</sup> and a direct introduction method.<sup>40),41)</sup> In the former case, the mobile phase solvents are removed before ionization, while in the latter the total effluent is introduced into the ion source. In both cases, a low concentration of the matrix is contained in the mobile phase to give efficient dispersion of the analyte in the matrix during the chromatographic separation. Eluent flow rates up to around 1 ml/min are applicable in the moving belt method, which allows the use of a conventional HPLC system with a 4.6-mm column. On the other hand, in the direct introduction method, the flow rate of the mobile phase introduced into the mass spectrometer is limited to 1–10  $\mu$ l/min.

The low concentration of the matrix, e.g., less than 10%, in the mobile phase does not have detrimental effect on the selectivity or the efficiency of HPLC.

The schematic diagram of the interface developed for micro-HPLC/FABMS is illustrated in Fig. 17.<sup>42)</sup> For this type of the interface it is important to maintain the amount of the matrix on the target, since this affects the stability and intensity of ionization. It is imagined that the mobile phase solvents evaporate rapidly, while the less-volatile matrix remains on the target and forms a thin layer.

The stability and intensity of ionization are greatly affected by the temperature of the interface because it alters the rate of consumption of the matrix. The temperature must, therefore, be kept constant by supplying the heat of evaporation. The top of the interface is attached to the copper plate so that the heat of the ion source block can be effectively transferred to the interface in order to give stable ionization.

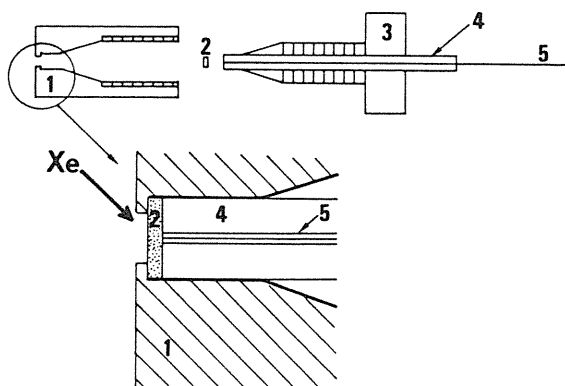


Fig. 17 Interface for micro-HPLC/FABMS.<sup>40)</sup> 1 = Modified union; 2 = porous filter; 3 = tough connector; 4 = stainless-steel tubing (0.25 mm ID  $\times$  1/16 in. OD); 5 = fused-silica tubing (41  $\mu$ m ID  $\times$  0.18 mm OD).

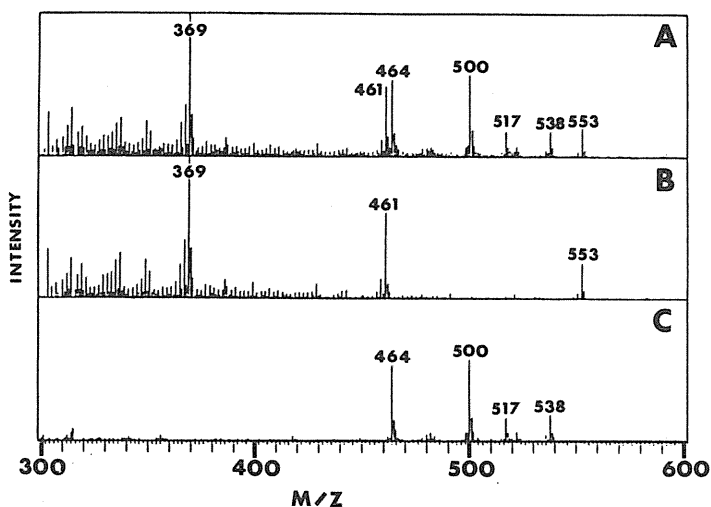


Fig. 18 Mass spectra of taurodeoxycholic acid.<sup>43)</sup> (A) Spectrum at the peak; (B) spectrum at the background; (C) subtracted spectrum A-B. Sample: ca. 40 ng.

The material and the thickness of the frit (or filter) affected the signal intensity in micro-HPLC/FABMS.<sup>42)</sup> Various materials such as stainless-steel, silver, glass, paper and PTFE with 70–300  $\mu$ m thickness were examined as the frit for the interface. A 70- $\mu$ m thick silver frit gave the best result, owing to its good wettability and lower dispersion of the analyte in the frit.<sup>42)</sup> Narrower peak volumes were observed for the thinner filters, demonstrating that additional band broadening caused by the filter is significant. A thickness of around 100  $\mu$ m is a compromise considering the mechanical strength.

A drawback of the off-line FABMS lies in great interference due to the matrix and the mobile phase solvents, leading to poor sensitivity in a low mass range. On-line FABMS

improves the sensitivity in the low mass range by subtraction of the background signals from the analyte signals.

Fig. 18 compares the mass spectra of taurodeoxycholic acid (M.W. = 499) corresponding to the peak (A), the background (B), and the subtracted spectrum (C) [ $A - B$ ].<sup>43)</sup> The background signals due to the matrix and the mobile phase solvents have been removed in the subtracted spectrum. This shows the stable ionization resulting from the micro-HPLC/FABMS system. The peaks at  $m/z = 464$ , 500, 517 and 538 correspond to  $[M - 2H_2O + H]^+$ ,  $[M + H]^+$ ,  $[M + NH_4]^+$  and  $[M + K]^+$ , where M represents the molecular species.

Applications of HPLC/FABMS cover bile acids,<sup>40),43)</sup> oligosaccharides,<sup>44)</sup> poly(ethylene glycols),<sup>42)</sup> antiamoebin I,<sup>39)</sup> emericimins,<sup>39)</sup> peptides<sup>41),45)-47)</sup> and nonionic detergents.<sup>48)</sup>

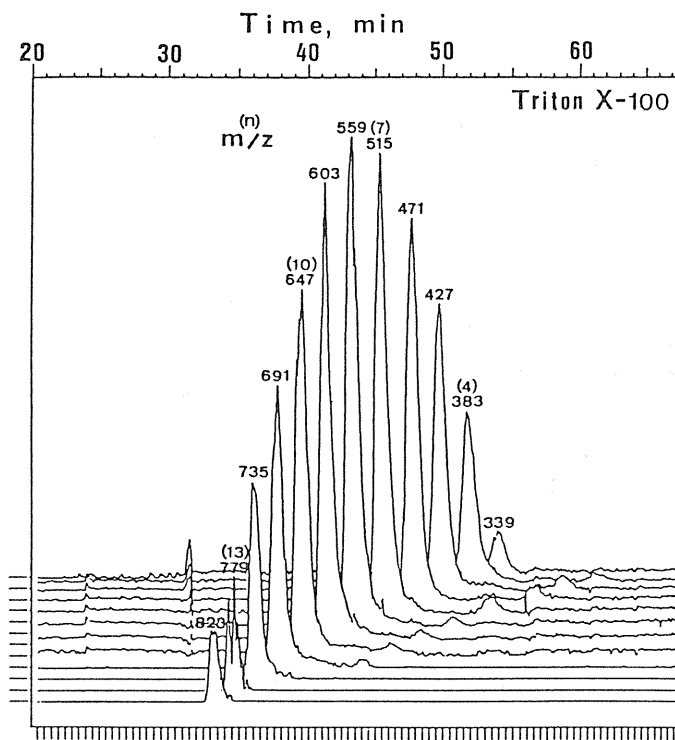


Fig. 19 Selected ion chromatograms of the components of Triton X-100.<sup>48)</sup> Column:  $200 \times 0.35$  mm ID packed with  $3\text{-}\mu\text{m}$  ODS. Mobile phase: acetonitrile-water-glycerol (55:40:5). Flow rate:  $2.1 \mu\text{l}/\text{min}$ . Sample:  $0.02 \mu\text{l}$  of 3% Triton X-100.

Fig. 19 demonstrates the selected ion chromatograms of Triton X-100 [tert.-octylphenyl-oligo(ethylene glycols)].<sup>48)</sup> A double-focusing type JMS-DX300 mass spectrometer was employed, and xenon atoms with 5 keV energy were used for ionization. The scan range was set at  $m/z$  150 to 900. Each  $m/z$  value corresponds to the protonated molecular ions. Oligomers with a degree of polymerization (DP) of 3–14 are observed in the selected ion chromatograms. Small peaks eluted after the main peaks may be structural isomers with different octylphenyl groups. Sub- to several nanograms are required to obtain a good spectrum.

HPLC/FABMS provides a strategy for the analysis of polar, thermally unstable, or large-molecular-weight compounds. The interfacing techniques developed for micro-HPLC/FABMS also work as an on-line, continuous sample introduction method for FABMS. The new interfaces reduce the problems encountered in sample handling in FABMS and save time. Although mass spectrometers with FAB ionization, as well as other ionization methods will work as versatile detectors for HPLC, the state of the art of HPLC/MS is still far from that of GC/MS. The interfacing techniques for HPLC/FABMS must be improved to increase the stability, reproducibility and repeatability of the signal intensity.

### 5.2. On-column detection

On-column detection has been originally proposed for micro-HPLC<sup>49),50)</sup> to eliminate the dispersion of analytes due to the connecting parts between the microcolumn and the detector's flow cell. However, the term "on-column detection" is used differently by different authors. In this article, on-column detection is defined as a case when the analytes are detected in the presence of a stationary phase. On the other hand, the term post-column detection is used for the case when the analytes are detected in the absence of the stationary phase. Since the stationary phase focuses the analytes in a partitioning zone, on-column detection has a potential to provide sensitivity increased by a factor of  $(1+k')$  in comparison with post-column detection, where  $k'$  is the capacity factor of the analytes.

The peak heights of the analytes decrease with increasing capacity factor in post-column detection :

$$h_{pi} = a\sqrt{N_i}/(1+k'_i) \quad (1)$$

where  $h_{pi}$  is a peak height of the analyte  $i$  in post-column detection,  $N_i$  is the number of theoretical plates for the component  $i$  and  $a$  is a constant. Assuming that only the focusing effect is involved, the concentration of the analyte in on-column detection is  $\psi(1+k'_i)/(1+\psi)$  times larger than that in post-column detection, where  $\psi$  is the phase ratio. Therefore, the peak height of the analyte observed in on-column detection,  $h_{oi}$ , is given by

$$h_{oi} = \epsilon\psi(1+k'_i)h_{pi}/(1+\psi) \quad (2)$$

where  $\epsilon$  is a coefficient accounting for the detection efficiency (cell volume, the percentage of the analyte irradiated by the excitation light, collection efficiency of fluorescence, etc.). Substituting  $h_{pi}$  in Eq. (1) into Eq. (2) yields :

$$h_{oi} = a\epsilon\psi\sqrt{N_i}/(1+\psi) \quad (3)$$

Eq. (3) indicates that the peak height in on-column detection is independent of the capacity factor. The theoretical plate number is usually approximately constant, independent of the capacity factor, in HPLC ( $k' \leq 10$ ). Thus the peak height of a solute is approximately constant of its capacity factor.

Fig. 20 demonstrates on-column and post-column fluorometric detection of sodium salicylate and aromatic hydrocarbons, in which the former analyte is not retarded on the stationary phase.<sup>51)</sup> It is evident that the peak heights of the retained solutes are enhanced for on-column detection.

The mass detection limits are compared in Table 2.<sup>51)</sup> The operating conditions are the same as in Fig. 20. It is clear that the mass detection limits are improved in on-column

Table 2. Mass detection limits at signal-to-noise ratio 2.<sup>52)</sup>

Analyte	Mass detection limits (pg)		Ratio of mass detection limits	$1 + k'$
	Post-column detection	On-column detection		
A	12	1.2	10	4.58
FL	32	2.6	12	5.27
9PA	1.7	0.11	15	7.87

detection. The larger the capacity factor, the larger is the improvement of the mass detection limit. It is certain that the detectability of the analyte eluted late is improved by on-column detection. The ratios of the mass detection limits are about two times larger than the values of  $(1 + k')$ , which indicates that the noise increases to a lesser extent in on-column detection. Another experiment also supported the result,<sup>52)</sup> in which the noise level was nearly the same for both on-column and post-column detection. The mass detection limit of 9-phenylanthracene was 0.11 pg at a signal-to-noise ratio of 2.

Fig. 21 illustrates the plots of  $h/\sqrt{N}$  versus the capacity factor.<sup>51)</sup> The capacity factor was changed by using different composition of the mobile phase. Peak heights divided by the square root of the plate number are plotted in order to compensate for the variation in the plate number with the capacity factor. The values of  $h/\sqrt{N}$  are nearly constant regardless of the capacity factor, as expected from Eq. (3).

It is somewhat inconvenient to fix the separation column in the detector. The use of a packed flow cell is alternative for on-column fluorometric detection.<sup>53)</sup> When the same stationary phase is used in the flow cell as in the separation column, the effects of the stationary phase on the signal intensity using the packed flow cell are essentially the same as in common on-column detection.

Fig. 22 demonstrates the on-column fluorometric detection of an artificial mixture of fatty acids (A) and total fatty acids in horse serum (B) using the packed flow cell.<sup>53)</sup> These fatty acids were derivatized with 9-anthryldiazomethane, and detected at 412 nm. In Fig. 22A ca. 4 pg each of the analytes were injected, and the mass detection limits were lower than 1 pg at a signal-to-noise ratio of 2.

On-column detection has a potential to improve the mass detection limits of the analytes eluted late, which is due to the focusing effect of the stationary phase. It should be noted that on-column fluorometric detection also has an environmental effect due to the stationary phase.<sup>54)</sup>

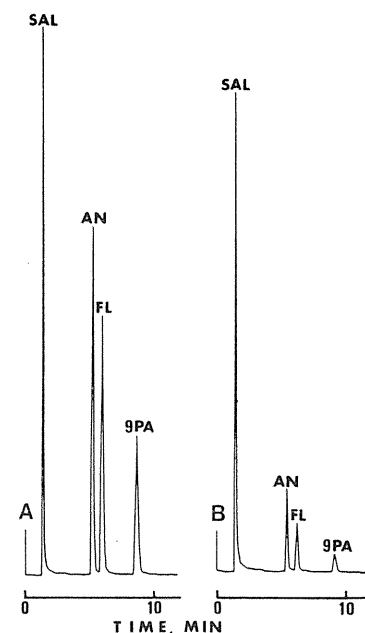


Fig. 20 On-column (A) and post-column (B) detection of sodium salicylate and aromatic hydrocarbons.<sup>51)</sup> Column:  $130 \times 0.34$  mm ID packed with  $5\text{-}\mu\text{m}$  ODS. Mobile phase: acetonitrile-water (80:20). Flow rate:  $4.2 \mu\text{l}/\text{min}$ . Samples: 3.3 ng of sodium salicylate (SAL); 2.5 ng of anthracene (AN); 3.0 ng of fluoranthene (FL) and 0.51 ng of 9-phenylanthracene (9PA). Detection wavelengths: excitation, 313 nm; emission, 420 nm. Detection volumes: on-column detection,  $0.14 \mu\text{l}$  ( $1.5 \text{ mm} \times 0.34 \text{ mm}$  ID); post-column detection,  $0.13 \mu\text{l}$  ( $2.5 \text{ mm} \times 0.26 \text{ mm}$  ID).

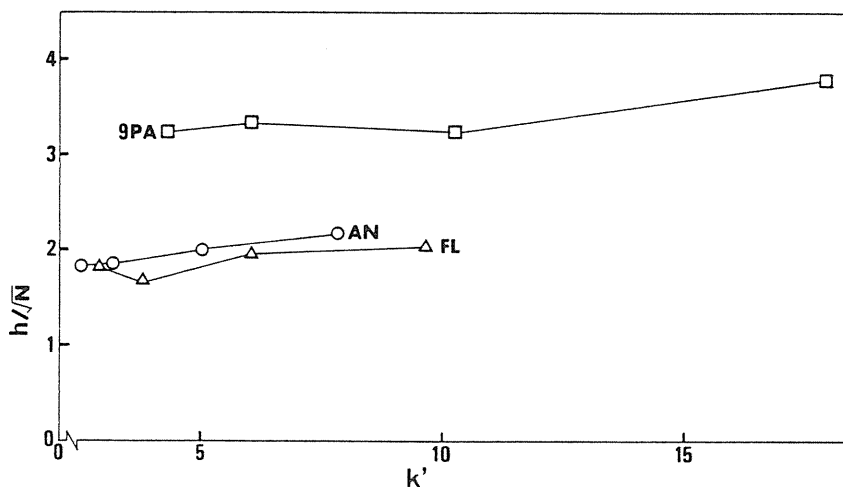


Fig. 21 Plots of  $h/\sqrt{N}$  (in arbitrary units) versus the capacity factor in on-column detection.<sup>51)</sup> Column:  $130 \times 0.34$  mm ID packed with  $5\text{-}\mu\text{m}$  ODS. Mobile phase: acetonitrile-water, 85:15; 80:20; 75:25 or 70:30. Detection wavelengths: excitation, 365 nm; emission, 430 nm.

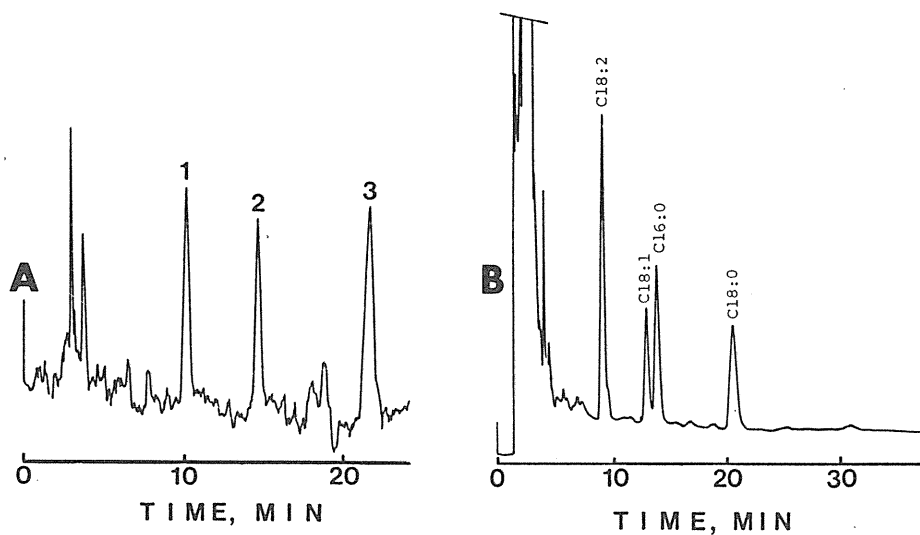


Fig. 22 On-column fluorometric detection of an artificial mixture of fatty acids (A) and total fatty acids in horse serum (B) using the packed flow cell.<sup>53)</sup> Column:  $100 \times 0.35$  mm ID packed with  $3\text{-}\mu\text{m}$  ODS. Mobile phase: acetonitrile-dichloromethane (90:10). Flow rate:  $4.2 \mu\text{l}/\text{min}$ . Flow cell:  $0.35$  mm ID. Effective flow cell length: (A)  $1.6$  cm; (B)  $1.3$  cm. Samples: (A) 1 =  $4.1$  pg of myristic acid, 2 =  $4.4$  pg of palmitic acid, 3 =  $4.1$  pg of stearic acid; (B) total fatty acids in horse serum. Wavelengths of detection: excitation, 365 nm; emission, 412 nm.

### 5.3. Indirect detection

Refractive index detectors have been employed as the universal detector in HPLC in spite of their poor sensitivity and inapplicability to gradient elution. However, the refractive index detectors for micro-HPLC are not commercially available yet. Indirect detection is alternative when adequate detectors are not available. It allows detection of ions (or ionic species) as well as uncharged species.<sup>55)</sup> Indirect UV detection in ion chromatography, which was initiated by Small and Miller,<sup>56)</sup> is one of the most successful application of indirect detection. Indirect detection is defined in this article as a case when transparent analytes are visualized by the variation of the background or by the detection of separate species produced by post-column interaction.

Indirect detection can be classified according to the type of the interaction between analytes and visualization agents: mobile-phase induced or post-column interaction.<sup>57)</sup>

#### Mobile-phase induced indirect detection

In this case, the mobile phase components visualizes analytes via interaction such as ion displacement, ion-pair formation, perturbation of partitioning process, etc. The mobile phase component maintains a background, and the analytes are detected owing to the variation of the background. Indirect UV detection in ion chromatography is an example of this case, in which analyte ions displace the mobile phase ions in order to maintain neutrality of the charge in the analyte band.<sup>56)</sup> Signal intensity of the induced peak in ion chromatography is easily estimated from the valences of the visualization agent and the analyte ion as well as the response factor of these species to the employed detector. The peak direction is generally negative in the indirect detection in ion chromatography.

In the indirect detection of uncharged species, induced peaks are mostly generated by perturbation of partition characteristics of the visualization agent due to analytes. Fig. 23 demonstrates the indirect UV detection of an artificial mixture of hydrocarbons (heptane to pentadecane) and components in kerosine using benzo[a]pyrene as the visualization agent.<sup>58)</sup> The retention time of the system peak, denoted as "S" in the figure, coincides with that of benzo[a]pyrene. The analytes eluted before the system peak give positive peaks, while those eluted after the system peak give negative peaks. The analytes eluted close to the system peak give larger signals.

It is more difficult to estimate the signal intensity in the indirect detection of uncharged species. Takeuchi et al.<sup>59)</sup> simulated the induced peak in the indirect detection of

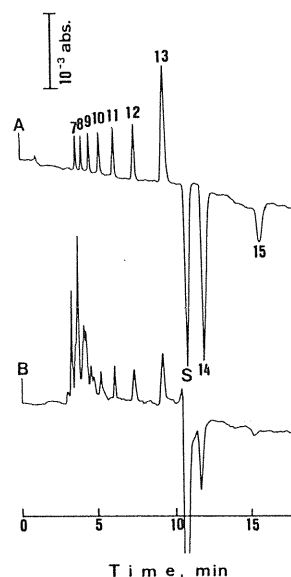


Fig. 23 Indirect UV detection of an artificial mixture of hydrocarbons and components in kerosine.<sup>58)</sup> Column: 150 × 0.34 mm ID packed with 5- $\mu$ m ODS. Mobile phase: methanol including  $1.2 \times 10^{-4}$  M benzo[a]pyrene. Flow rate: 4.2  $\mu$ l/min. Samples: (A) 0.5% (v/v) each, the numbers correspond to the carbon numbers of straight-chain hydrocarbons; (B) 6.7% (v/v) kerosine. Wavelength of UV detection: 300 nm.



uncharged species and proposed an simulated equation:

$$S = FC_{a0} W_{b0} c \cdot \frac{\phi}{\phi + 1} \cdot \frac{k'_a(k'_b + 1)}{k'_b - k'_a} \quad (4)$$

where  $S$  is the peak area of the induced peak,  $F$  is a response factor,  $C_{a0}$  is the concentration of the visualization agent,  $W_{b0}$  is the amount of the analyte injected,  $c$  is the coefficient accounting for a degree of the variation of the capacity factor of the visualization agent,  $\phi$  is the phase ratio,  $k'_a$  and  $k'_b$  are the capacity factors of the visualization agent and the analyte.  $c$  is usually negative, and Eq. (4) gives negative peak areas for negative peaks. Eq. (4) indicates that the peak area of the analyte increases with increasing  $k'_a$  and  $k'_b$  and decreasing a difference between  $k'_a$  and  $k'_b$ . This means that the detection limit of the analyte can be improved by the careful selection of the operating conditions. Eq. (4) also explains the change of the peak direction of the induced peak depending on the eluted position.

Hydrocarbons (pentane, hexane and heptane) were separated in the reversed-phase mode, and detected by indirect photometry. Chrysene was employed as the visualization agent, and by changing the mobile phase composition (acetonitrile-water) different capacity factors of the hydrocarbons were obtained. In this case,  $c$  was negative. Fig. 24 shows the relationship between the peak areas and  $k'_a(k'_b + 1) / |k'_a - k'_b|$ .<sup>59)</sup> A good linear relationship is observed even if the value of  $c$  is not considered. The  $c$  value of the analyte depends on the chemical and physical properties of the mobile and stationary phase and the analyte itself.

It should be noted that the column temperature should be kept constant. Otherwise, the baseline noise becomes severe because the variation of the column temperature leads to variation of the partition coefficient of the visualization agent. Temperature of microcolumns can easily be controlled because of their low heat capacity.

Cyclodextrins can be indirectly detected based on another detection principle. Frijlink et al.<sup>60)</sup> reported that the colour intensity of phenolphthalein decreased owing to inclusion complexation into cyclodextrins and that it was able to visualize  $\beta$ - and  $\gamma$ -cyclodextrin based on

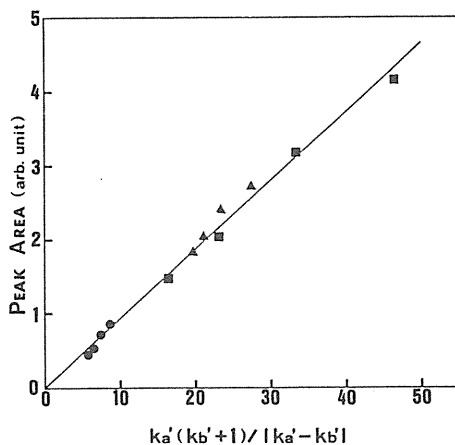


Fig. 24 Relationship between the peak area and  $k'_a(k'_b + 1) / |k'_a - k'_b|$ .<sup>59)</sup> Column: 100 × 0.26 mm ID packed with 3- $\mu$ m ODS. Mobile phase: acetonitrile-water = 95:5, 90:10, 85:15 or 80:20 containing  $8 \times 10^{-5}$  M chrysene. Flow rate: 2.1  $\mu$ l/min. Sample:  $\bullet$ , pentane;  $\blacktriangle$ , hexane;  $\blacksquare$ , heptane, 0.5% (v/v) of each was injected.

that principle in HPLC. The stability constant of the inclusion complex for  $\beta$ -cyclodextrin is larger than that for  $\gamma$ -cyclodextrin, which means that the former is expected to be detected better than the latter.

The indirect detection of  $\beta$ - and  $\gamma$ -cyclodextrin is demonstrated in Fig. 25.<sup>61)</sup> The positive peak eluted in 13 min, denoted as "S" in the figure is the system peak, the retention time of which coincides with that of phenolphthalein. The peak area of  $\beta$ -cyclodextrin was larger than that of  $\gamma$ -cyclodextrin although the former eluted apart from the system peak, supporting that the cyclodextrin were visualized via the inclusion complexation. Actually, they were visualized by both inclusion complexation and perturbation of partition of phenolphthalein.

#### Post-column induced indirect detection

Post-column interaction generates the separate species corresponding to the analytes, which are subjected to adequate detection. In this case, the visualization agents are loaded on the post-column or detectable species are produced by the post-column interaction, and the

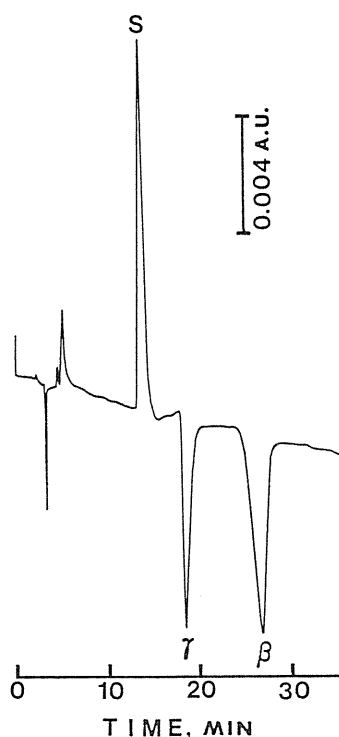


Fig. 25 Indirect photometric detection cyclodextrins.<sup>61)</sup> Column:  $100 \times 0.35$  mm ID packed with  $3\text{-}\mu\text{m}$  ODS. Mobile phase:  $0.3$  mM phenolphthalein dissolved in  $3\%$  methanol solution with pH  $12.2$ . Flow rate:  $2.8$   $\mu\text{l}/\text{min}$ . Samples:  $\beta = \beta$ -cyclodextrin;  $\gamma = \gamma$ -cyclodextrin,  $0.04$   $\mu\text{g}$  each was injected. Wavelength of detection:  $550$  nm.

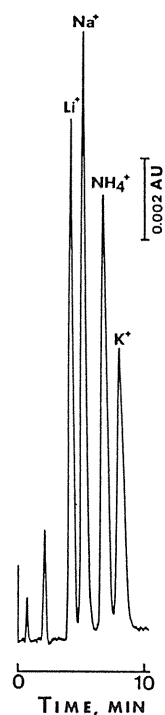


Fig. 26 Indirect UV detection of an artificial mixture of monovalent cations using  $\beta\text{NS}$  as the chromophoric ion.<sup>63)</sup> Columns: IC-Cation ( $50 \times 0.35$  mm ID), Suppressor ( $\text{OH}^-$ -form,  $40 \times 0.35$  mm ID); ion-replacement column ( $\beta\text{NS}$ -form,  $30 \times 0.35$  mm ID), connected in series. Eluent:  $2$  mM nitric acid. Flow rate:  $2.8$   $\mu\text{l}/\text{min}$ . Samples:  $1$  mM each. Wavelength of UV detection:  $225$  nm.

mobile phase component does not generally provide any background. Post-column ion-replacement in ion chromatography and enzyme reaction can be involved in this case.

An example of the former case is dual-column ion chromatography with ion-replacement.<sup>62)-64)</sup> When the analyte ion passes through the post-suppressor ion-replacement column (or membrane), it coelutes with the reagent ion with opposite charge, or displaces the reagent ion with the same charge. When the reagent ion is detectable, the analyte ion can be indirectly detected.

Fig. 26 demonstrates the indirect UV detection of an artificial mixture of monovalent cations via post-suppressor ion replacement.<sup>63)</sup> Separation, suppressor (OH<sup>-</sup>-form) and post-suppressor ion-replacement columns are connected in series.  $\beta$ -naphthalenesulphonate ( $\beta$ NS) is loaded on the ion-replacement column as the chromophoric ion. The analyte cations coelute with  $\beta$ NS from the ion-replacement column and are detected at 225 nm.

Various organic compounds are indirectly detected after post-column enzyme reaction. The enzyme reaction commonly produces hydrogen peroxide or NADH, which is subjected to adequate detection. This type reaction is generally specific and sensitive. Fluorometric detection of bile acids shown in Chapter 4.2 is a typical example.

## 6. Open-tubular capillary LC

Open-tubular columns were originally proposed by Golay<sup>65)-67)</sup> for use in GC and have been widely utilized. In GC, open-tubular columns have a good permeability and consequently produce higher theoretical plate numbers per unit time and unit pressure drop across the column than packed columns. Open-tubular columns producing higher theoretical plate numbers can resolve complex mixtures, which are difficult to separate on conventional packed columns. Due to their high resolution, the usefulness of open-tubular columns in LC has been investigated.

Open-tubular columns, with the same dimension as in GC, were employed in LC, but they gave poor column efficiencies, due to low diffusion speed in a liquid mobile phase.<sup>68)-70)</sup> It has been theoretically proven that narrow-bore columns should be employed in LC and Ishii's group<sup>70)</sup> first showed the feasibility of open-tubular LC using 60- $\mu$ m ID columns.

The magnitude of the dispersion of a solute in laminar flow is too large in LC, which necessitates the use of narrow-bore columns. Thus, research has been directed toward the modification of the laminar flow in the open-tubular column. Operation in the turbulent flow region, flow segmentation with air plugs, the use of helically coiled columns or deformed or wavy tubes, and the use of electroosmosis flow have been investigated. Most recent research on open-tubular capillary LC has dealt with narrow-bore columns.

### 6.1. Theoretical aspects

The basic equation for open-tubular capillary LC was derived by Golay.<sup>67)</sup>

$$H = \frac{2 D_m}{u} + \frac{(11 k'^2 + 6 k' + 1) d_c^2}{96 (1 + k')^2 D_m} u + \frac{2 k' d_f^2}{3 (1 + k')^2 D_s} u \quad (5)$$

where  $H$  is the plate height,  $u$  is the linear velocity of the mobile phase,  $k'$  is the capacity

factor,  $d_c$  is the column diameter,  $d_f$  is the thickness of the stationary phase film and  $D_m$  and  $D_s$  are the diffusion coefficients of a solute in the mobile and stationary phases, respectively. The first term on the right hand side of Eq. (5) is due to longitudinal molecular diffusion, while the second and third terms are due to the resistance to mass transfer in the mobile and stationary phases, respectively. The diffusion coefficient of a solute in a liquid is much smaller than that in a gas, resulting in large contribution of the second term in LC.

Decreasing the contribution of the second term to the plate height plays an important role in achieving good results with open-tubular columns. In order to reduce the contribution of the resistance to mass transfer in the mobile phase, narrow-bore open-tubular columns should be operated under conditions achieving large diffusivity, i.e., operated at higher column temperatures and with low-viscosity mobile phases.

Jorgenson and Guthrie<sup>71)</sup> derived an equation describing  $N$  values of the last eluting component as a function of column radius, given the constraints on retention time and pressure.

$$N = \frac{24(1+k')D_m P t r^2}{384(1+k')D_m^2 \eta t + (1+6k'+11k'^2)Pr^4} \quad (6)$$

where  $P$  is the pressure drop,  $t$  is the retention time,  $r$  is the column radius and  $\eta$  is the viscosity of the mobile phase, respectively.

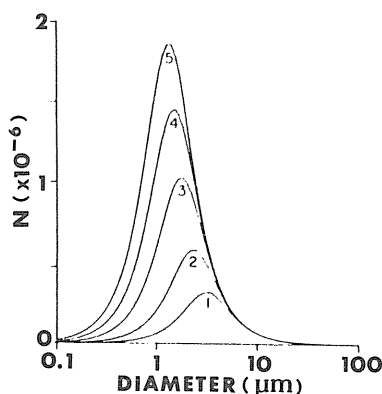


Fig. 27 Number of theoretical plates as a function of column diameter for five different pressures.<sup>71)</sup>  $k' = 10$ ,  $D_m = 1 \times 10^{-5}$  cm<sup>2</sup>/sec,  $\eta = 5 \times 10^{-3}$  poise,  $t = 2$  hr. 1 = 21 bar; 2 = 69 bar; 3 = 210 bar; 4 = 420 bar; 5 = 690 bar.

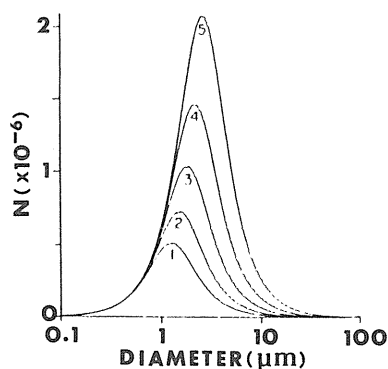


Fig. 28 Number of theoretical plates as a function of column diameter for five different analysis time.<sup>71)</sup>  $k' = 10$ ,  $D_m = 1 \times 10^{-5}$  cm<sup>2</sup>/sec,  $\eta = 5 \times 10^{-3}$  poise,  $P = 210$  bar. 1 = 0.5 hr; 2 = 1.0 hr; 3 = 2.0 hr; 4 = 4.0 hr; 5 = 8.0 hr.

Figs. 27 and 28 illustrate the relationships between these parameters.<sup>71)</sup> It should be noted that somewhere between 1 and 2  $\mu\text{m}$  of the optimum column diameter for columns over wide range of operating pressures and analysis times.

They further derived equations which give optimum diameters and lengths when limits are placed on the available pressure and analysis time:<sup>71)</sup>

$$r_{\text{opt}} = \left[ \frac{384 D_m^2 \eta (1 + k') t}{(1 + 6 k' + 11 k'^2) p} \right]^{1/4} \quad (7)$$

$$L_{\text{opt}} = \left[ \frac{6 D_m^2 P t^3}{(1 + k') (1 + 6 k' + 11 k'^2) \eta} \right]^{1/4} \quad (8)$$

where  $r_{\text{opt}}$  and  $L_{\text{opt}}$  are the optimum radius and length, respectively.

Finally, by substituting the optimum value for radius from Eq. (7) into Eq. (6) we get the maximum number of theoretical plates attainable with these pressure and time restrictions

$$N_{\text{max}} = \left[ \frac{3 P (1 + k') t}{8 \eta (1 + 6 k' + 11 k'^2)} \right]^{1/2} \quad (9)$$

where  $N_{\text{max}}$  is the maximum number of theoretical plates.

## 6.2. Performance of open-tubular columns

### Preparation procedures<sup>72)</sup>

Soda-lime glass capillaries were drawn with a GDM-1B glass-drawing machine (Shimadzu, Kyoto, Japan) and treated with 1 *N* sodium hydroxide solution at 35 to 55°C for 2 days. The capillaries were washed with methanol until the effluent from the column became neutral. After washing with methanol, the capillaries were dried under helium at 120°C for 2 to 4 hr, then washed with 0.01 *N* hydrochloric acid in methanol, distilled water, and then with methanol. Finally, they were dried under helium at 120°C for 2 hr.

This treatment generated a stable silica gel layer on the glass surface and thus substantially increased the surface area of the capillaries. This characteristic allows the introduction of large amounts of stationary phase than a smooth glass surface.

Structures of prepared chemically-bonded stationary phases are illustrated in Fig. 29.<sup>72)</sup> Silane reagents are shown as reacting monofunctionally with silanol groups, but in practice some reagents react bifunctionally. Wall-coated columns can also be used as the separation column for LC if the mobile phase is saturated with the stationary phase.

### Instrumentation

Chromatographs for open-tubular capillary LC are not available commercially. These columns have a quite small inner volume, e.g., a 5 m × 50 μm ID column has a volume of about 10 μl. When such capillary columns are used as the separation columns, the extra-column effect becomes serious. Flow rates lower than 1 μl/min are required in most cases in open-tubular capillary LC. There is no LC pump that can supply the mobile phase at such a low flow rate. Both injection and detection volumes should be quite small, sometimes less than 10 nl. Thus, the apparatus must be designed by each laboratory.

### Wall-coated columns

The dynamic coating method is more convenient for coating the liquid phase onto the

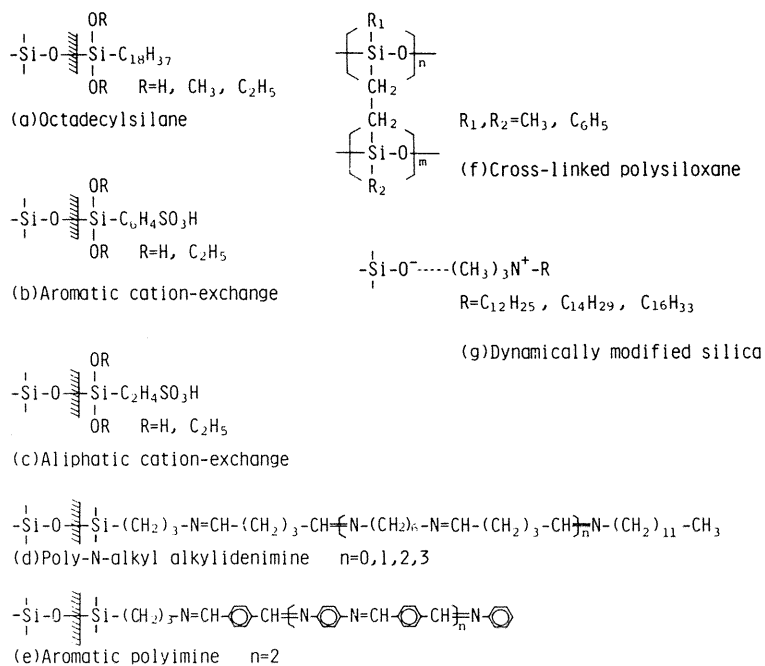
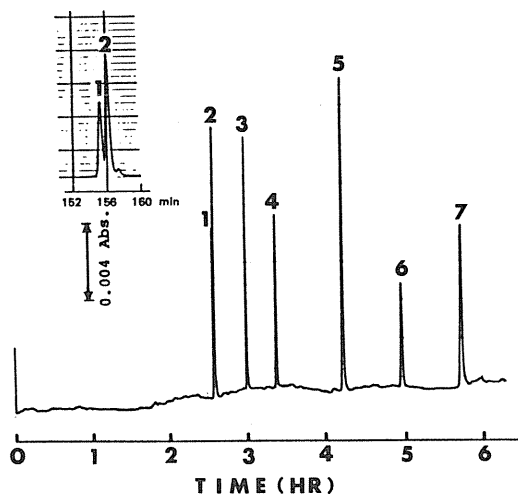
Fig. 29 Structures of non-extractable stationary phases.<sup>72)</sup>

Fig. 30 Separation of aromatic amines on an open-tubular column.<sup>73)</sup> Column: 20 m  $\times$  37  $\mu\text{m}$  ID coated with  $\beta$ - $\beta'$ -oxydipropionitrile. Mobile phase: hexane. Flow rate: 0.14  $\mu\text{l}/\text{min}$ . Peak identification ( $k'$ ,  $N$ ): 1 = isooctane (0, 740,000); 2 = *N*, *N*-diethylaniline (0.006, 610,000); 3 = *N*-phenyl- $\alpha$ -naphthylamine (0.17, 450,000); 4 = *N*-phenyl- $\beta$ -naphthylamine (0.31, 360,000); 5 = aniline (0.64, 320,000); 6 =  $\alpha$ -naphthylamine (0.92, 250,000); 7 =  $\beta$ -naphthylamine (1.22, 200,000). Wavelength of UV detection: 230 nm.

narrow-bore capillary tubing than is the static coating method. Since the thickness of the stationary phase film in the dynamic method is affected by the coating speed, it is important to keep the speed constant in order to obtain good column efficiencies. The coating speed can be kept constant by attaching a buffer capillary tubing to the actual capillary column. The diameter of the buffer capillary should be the same as that of the actual column.

Fig. 30 shows the separation of aromatic amines on a  $20\text{ m} \times 37\text{ }\mu\text{m}$  ID column coated with  $\beta$ - $\beta'$ -oxydipropionitrile.<sup>73)</sup> Seven hundred forty thousand (740,000) theoretical plates were produced for the unretained solute in 155 min and 200,000 theoretical plates were produced for the peak of  $k' = 1.22$ . The peak at  $k' = 0.006$  (peak 2) is separated from the solvent peak ( $k' = 0$ ).

Fig. 31 shows the rapid separation of xylene isomers on a short open-tubular column using liquid propane as the mobile phase, with linear velocity of  $11\text{ cm/sec}$ .<sup>74)</sup> The separation is carried out in 2 min.

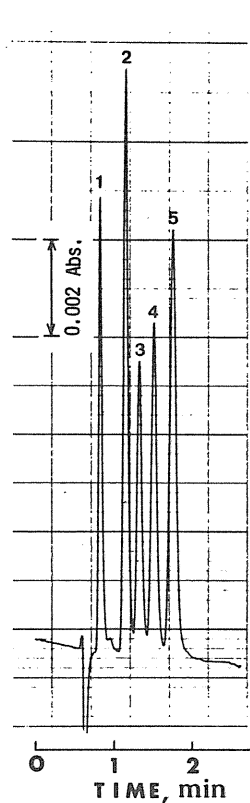


Fig. 31 Rapid separation of xylene isomers on a short open-tubular column using liquid propane as the mobile phase.<sup>74)</sup> Column:  $3.4\text{ m} \times 33\text{ }\mu\text{m}$  ID, coated with  $\beta$ ,  $\beta'$ -oxydipropionitrile. Mobile phase: liquid propane. Flow rate:  $5.6\text{ }\mu\text{l/min}$ . Samples: 1 = 2, 6-xylene; 2 = 2, 5-xylene; 3 = 2, 3-xylene; 4 = 3, 5-xylene; 5 = 3, 4-xylene. Wavelength of UV detection: 280 nm.

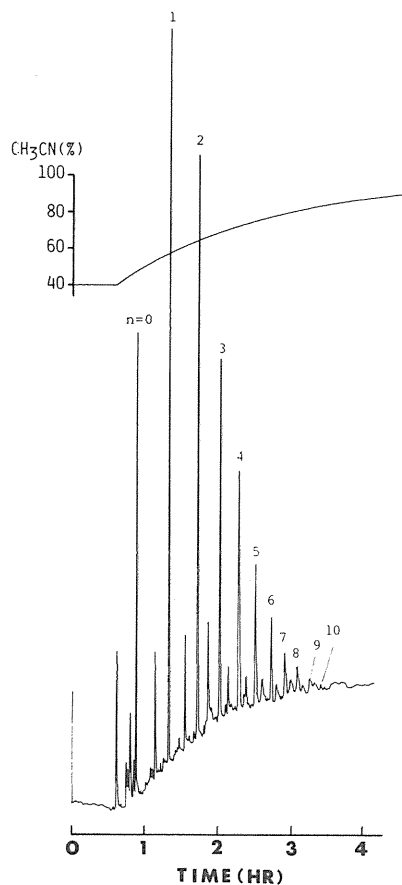


Fig. 32 Solvent-gradient separation of epoxy resin oligomers.<sup>75)</sup> Column: ODS,  $22\text{ m} \times 31\text{ }\mu\text{m}$  ID. Mobile phase: acetonitrile-water, gradient profile as indicated. Flow rate:  $0.52\text{ }\mu\text{l/min}$ . Sample: 160 ng of Epikote 1001. Column temperature:  $44^\circ\text{C}$ . Wavelength of UV detection: 225 nm.

### *Non-extractable stationary phases*

Chemically-bonded, cross-linked and dynamically-modified stationary phases have been prepared for open-tubular capillary LC. These non-extractable stationary phases permit solvent-gradient elution and facilitate temperature programming.

Fig. 32 demonstrates a solvent-gradient separation of epoxy resin oligomers. Besides the main peaks, many of by-products are resolved on the ODS capillary column.<sup>75)</sup>

The performance of capillary columns of 30 to 50  $\mu\text{m}$  ID was somewhat poorer than that of packed columns. However, these microcolumn techniques will help to prepare narrow-bore open-tubular columns with non-extractable stationary phases.

## 7. Approach to SFC and GC: Unified chromatography

Chromatographic separation modes are classified by the physical state of the mobile phase in the column, for example, LC and GC. Supercritical fluid chromatography (SFC) is now recognized as an intermediate separation method between LC and GC, its chromatographic properties originate from its characteristic mobile phase, high-density gas. The physical properties of the mobile phase can be regulated by both temperature and pressure. In other words, the separation mode can be selected by changing the column temperature and the pressure in the column. Mobile phase delivery, injection, separation, detection systems must be developed so that the different mode (LC, SFC, or GC) can be selected by using a single chromatographic system. Moreover, the different-mode separations can be carried out in series in a single chromatographic run by the careful selection of the operating conditions. This is the concept of unified chromatography.<sup>76),77)</sup>

Open-tubular and packed capillary columns facilitate the demonstration of these different-mode separations with a single chromatographic system because mass flow rates for these capillary columns are convenient to hyphenate with various types of detectors. Each separation mode can be optimized by the careful selection of the type of separation column and stationary phase, column dimensions, mobile phase, detector, and operating conditions.

Fig. 33 shows plots of the logarithms of the capacity factor ( $\log k'$ ) of aromatic hydrocarbons versus the reciprocal of the absolute column temperature ( $1/T$ ) using a packed column and a carbon dioxide mobile phase. The critical temperature and pressure of carbon dioxide are 31°C and 75 kgf/cm<sup>2</sup>, respectively. The inlet pressure was kept at 120 kgf/cm<sup>2</sup>. The supercritical temperature of carbon dioxide is denoted as "CT" in the figure. Convex curves were observed in the supercritical temperature region. As the column temperature increased, the capacity factor increased in the lower supercritical temperature region, but decreased at high column temperatures. In the latter region, linear relationships between two parameters were observed.

The region in which the capacity factor decreased with increasing column temperature is defined in this article as the GC-like SFC region, while the region in which the capacity factor increased with increasing column temperature is defined as LC-like SFC region. The results in Fig. 33 indicate that different retention mechanisms were involved in the supercritical temperature region, where contributions of volatility of the analytes and solvation of the analytes due to the mobile phase were combined. These two contributions depended differently on column temperature and pressure. The volatility contribution increased with increasing column temperature, while the solvation increased with decreasing column temperature and with increasing pressure in the column. In other words, the volatility contribution to retention of the analyte was dominant in the GC-like SFC region, while the solvation contribution was dominant in the LC-like SFC region.



The profile of the relationship between  $\log k'$  and  $1/T$  observed in Fig. 33 varied with the pressure in the column. For example, the GC-like SFC region appeared at lower column temperature at lower pressures. The profile was also varied by the solvent employed as the mobile phase.

Fig. 34 shows the relationships between  $\log k'$  and  $1/T$  using hexane as the mobile phase.<sup>78)</sup> The inlet pressure was kept at 5 kgf/cm<sup>2</sup>, while the outlet pressure was released to ambient pressure. Even when the pressure was not applied to the outlet of the column, an atmospheric pressure plus the pressure drop across the connecting parts between the column outlet and the flow cell of the detector are still applied to the column outlet. This is the reason why the mobile phase is liquid when passing through the flow cell of the UV detector in the examined temperature region. The critical temperature and pressure of hexane are 234°C and 30.6 kgf/cm<sup>2</sup>, respectively. The critical temperature of hexane is denoted as "CT" in the figure. At higher temperature linear relationships between two parameters are observed. Since the applied pressure is

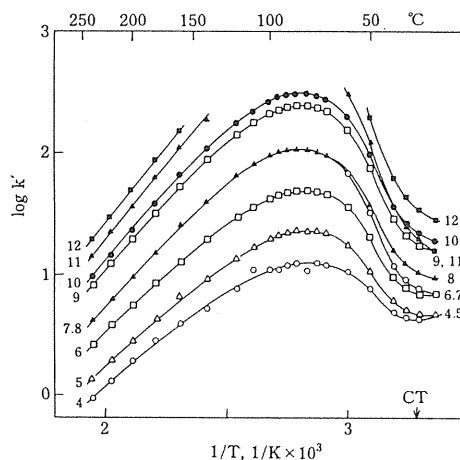


Fig. 33 Log  $k'$  versus the reciprocal absolute column temperature. Column:  $145 \times 0.3$  mm ID packed with  $5\text{-}\mu\text{m}$  ODS. Mobile phase: carbon dioxide. Inlet pressure:  $120\text{ kgf/cm}^2$ . Samples 4 = naphthalene; 5 = biphenyl; 6 = fluorene; 7 = *o*-terphenyl; 8 = anthracene; 9 = fluoranthene; 10 = pyrene; 11 = 9-phenylanthracene; 12 = triphenylene.

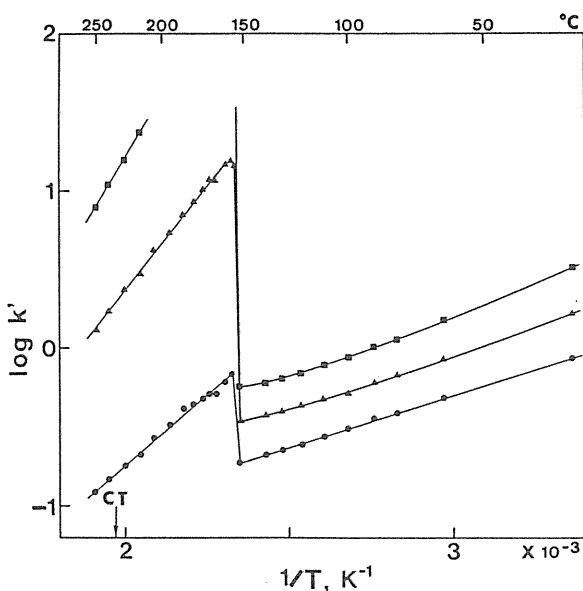


Fig. 34 Log  $k'$  versus the reciprocal absolute column temperature.<sup>78)</sup> Column:  $300 \times 0.5$  mm ID packed with  $10\text{-}\mu\text{m}$  silica gel. Mobile phase: hexane. Inlet pressure:  $5\text{ kgf/cm}^2$ . Outlet pressure: ambient pressure. Samples:  $\circ$  = benzene;  $\blacktriangle$  = naphthalene;  $\blacksquare$  = biphenyl.

lower than the critical pressure, the hexane vaporizes at temperature lower than the critical temperature. When the outlet pressure is higher than the vapor pressure at the operated temperature, the hexane is liquid in the column and analytes are separated in the normal-phase LC mode; almost linear relationships between two parameters are observed.

At intermediate temperature the capacity factor drastically changes with column temperature, where the state of the hexane in the column changes from liquid to gaseous in the direction of the current of a stream, and both liquid and gaseous hexane exist at the boundary region in the column. In other words, the retention observed at the intermediate temperature is attributed to contributions due both to LC and GC separation process in the single column.

These results indicate that positive-temperature programming is promising in GC-like SFC and in LC, while negative-temperature programming is promising in LC-like SFC and it replaces a part of well-known pressure programming in SFC. By the selection of the column temperature and the pressure, LC, SFC, and GC modes can be selected with a single chromatographic system. Moreover, different separation modes can be carried out in series in a single chromatographic run.

Fig. 35 demonstrates GC separation of components of a light oil using a carbon dioxide carrier gas and a micropacked columns for LC.<sup>79)</sup> The column temperature was 35°C for the initial 5 min, then programmed to 230°C at a rate of 5°C/min, and hold at 230°C.

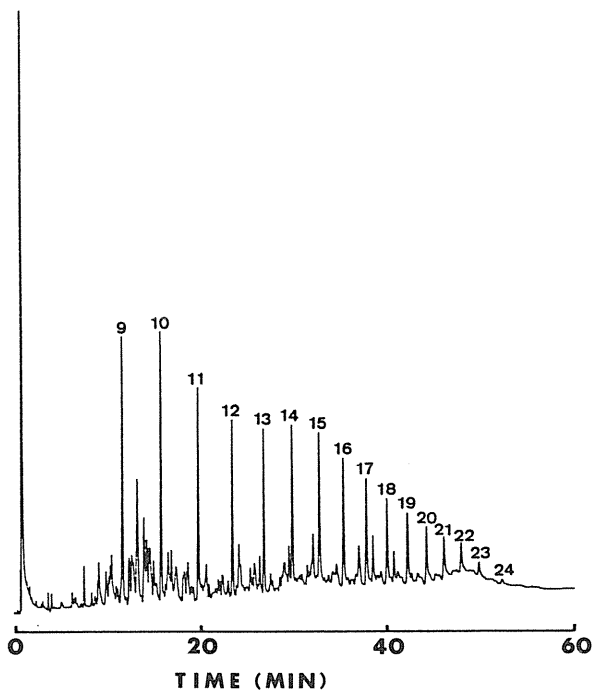


Fig. 35 GC separation of components of a light oil.<sup>79)</sup> Column: 300 × 0.3 mm ID packed with 5- $\mu$ m ODS. Carrier: carbon dioxide. Inlet pressure: 63 kgf/cm<sup>2</sup>. Outlet pressure: ambient. Column temperature: 5 min initial isothermal period at 35°C, then temperature programmed at 5°C/min, and held at 230°C. Sample: light oil diluted twice with pentane. The numbers in the figure refer to the carbon numbers of the corresponding straight-chain hydrocarbons. Injection volume: 0.02  $\mu$ l. Detector: flame ionization detector (FID).

Straight-chain hydrocarbons were identified by the retention times of a reference sample. Straight-chain hydrocarbons with carbon numbers of 9–24 were observed together with many other peaks. The separation was carried out on the  $300 \times 0.3$  mm ID column packed with  $5\text{-}\mu\text{m}$  ODS, and the resolution achieved with this system was slightly poorer than the resolution achieved on a common open-tubular capillary column of  $25\text{ m} \times 0.25$  mm ID, but better than or comparable to the resolution obtained on packed columns commonly used in GC.

Fig. 36 demonstrates the SFC separation of components of OV-17 on a silica gel packed column using diethyl ether as the mobile phase.<sup>80)</sup> The separation was carried out by the pressure programming. The critical temperature and pressure of diethyl ether are  $194^\circ\text{C}$  and  $36.8\text{ kgf/cm}^2$ . The pressure drop across the separation column was kept constant at  $5\text{ kgf/cm}^2$ .

Fig. 37 demonstrates the unified fluid chromatographic separation of an artificial mixture of aromatic hydrocarbons and styrene oligomers on a silica gel packed column using diethyl

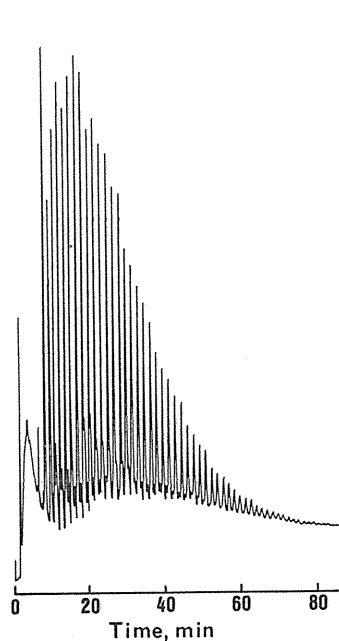


Fig. 36 SFC separation of methylphenylsiloxane oligomers on a silica gel column using diethyl ether as the mobile phase.<sup>80)</sup> Column:  $300 \times 0.5$  mm ID packed with  $5\text{-}\mu\text{m}$  ODS. Initial inlet pressure:  $45\text{ kgf/cm}^2$ . Pressure programmed at  $2\text{ kgf/cm}^2$  for 5 min, at  $1\text{ kgf/cm}^2$  for the next 5 min, and at  $0.5\text{ kgf/cm}^2$  for the rest of the analysis. Pressure drop:  $5\text{ kgf/cm}^2$ . Temperature:  $230^\circ\text{C}$ . Sample: OV-17 dissolved in tetrahydrofuran. Wavelength of UV detection:  $215\text{ nm}$ .

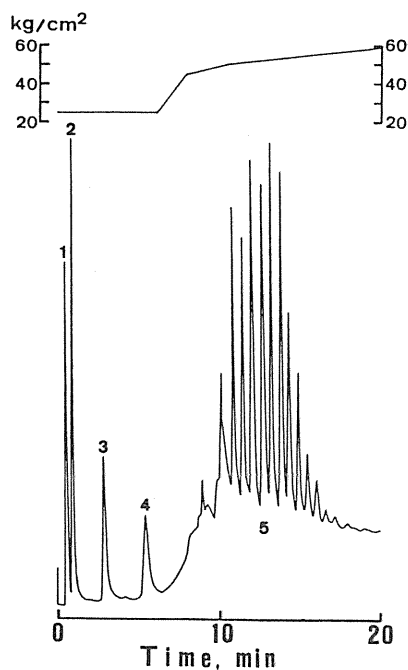


Fig. 37 Separation of an artificial mixture of aromatic hydrocarbons and styrene oligomers on a packed silica gel column.<sup>76)</sup> Column:  $150 \times 0.5$  mm ID packed with  $5\text{-}\mu\text{m}$  silica gel. Mobile phase: diethyl ether. Inlet pressure: programmed as shown in the figure. Pressure drop:  $5\text{ kgf/cm}^2$ . Temperature:  $220^\circ\text{C}$ . Samples: 1 = benzene; 2 = naphthalene; 3 = anthracene; 4 = pyrene; 5 = polystyrene A-1000 (weight-average molecular weight = 950). Wavelength of UV detection:  $220\text{ nm}$ .

ether as the mobile phase.<sup>76)</sup> These analytes were isothermally separated at supercritical temperature (220°C), and the pressure was programmed so that the aromatic hydrocarbons were separated by the GC mode prior to the SFC separation of the styrene oligomers. The aromatic hydrocarbons were separated at subcritical pressure, the inlet and outlet pressures being kept at 25 and 20 kgf/cm<sup>2</sup>, respectively. The styrene oligomers were then separated by the pressure programming as shown in the figure. This type of separation will be of practical importance when the sample contains compounds with wide-ranging volatilities.

## 8. Future prospects of microcolumn chromatography

Attractive features of micro-HPLC described in Chapter 2 were experimentally demonstrated in this article. Nevertheless, reliable micro-HPLC systems have never been appeared in the market, and conventional HPLC is still leading in this field. This is because micro-HPLC still possesses several problems to be solved. For example, reliable pumping systems running at very low flow rates (1–10  $\mu$ l/min), solvent-gradient systems at such low flow rates; injection systems which make a good use of trace amounts of samples; and sensitive, universal detection systems comparable to FID in GC are not commercially available (the last problem is also encountered in conventional HPLC). These problems must be solved before micro-HPLC is appreciated by lots of chromatographers.

Microcolumn separations and ancillary techniques developed for LC, however, have been successfully applied to SFC, GC and capillary electrophoresis. These capillary separation methods have numerous merits, and have been a well-recognized direction in science and technology as modern electronics and computer technology have been primarily based on miniaturization.

## References

- 1) M. Tswett, Ber. Deutsch. Botan. Ges., **24**, 316 (1906).
- 2) D.T. Day, Proc. Am. Phil. Soc., **36**, 112 (1897).
- 3) C.G. Horváth, B.A. Preiss and S.R. Lipsky, Anal. Chem., **39**, 1422 (1967).
- 4) R.P.W. Scott and P. Kucera, J. Chromatogr., **125**, 251 (1976).
- 5) D. Ishii, JASCO Report, **11** (6), 1 (1974).
- 6) R.P.W. Scott (editor), "Small Bore Liquid Chromatography Columns: their Properties and Uses", John Wiley & Sons, New York, 1984.
- 7) P. Kucera (editor), "Microcolumn High-Performance Liquid Chromatography", Elsevier, Amsterdam, 1984.
- 8) M. Novotny and D. Ishii (editors), "Microcolumn Separations", Elsevier, Amsterdam, 1985.
- 9) D. Ishii (editor), "Introduction to Microscale High-Performance Liquid Chromatography", VCH Publishers, New York, 1988.
- 10) T. Takeuchi and D. Ishii, J. Chromatogr., **213**, 25 (1981).
- 11) T. Takeuchi and D. Ishii, J. High Resolut. Chromatogr. Commun., **4**, 469 (1981).
- 12) T. Takeuchi, Y. Jin and D. Ishii, J. Chromatogr., **321**, 159 (1985).
- 13) D. Ishii, K. Watanabe, H. Asai, Y. Hashimoto and T. Takeuchi, J. Chromatogr., **332**, 3 (1985).
- 14) M. Goto, Y. Koyanagi and D. Ishii, J. Chromatogr., **208**, 261 (1981).
- 15) A.L. Knecht, E.J. Guthrie and J.W. Jorgenson, Anal. Chem., **56**, 479 (1984).
- 16) M. Goto, E. Sakurai and D. Ishii, J. Liq. Chromatogr., **6**, 1907 (1983).
- 17) Y. Ito, T. Takeuchi, D. Ishii and M. Goto, J. Chromatogr., **346**, 161 (1985).

- 18) T. Takeuchi and D. Ishii, *J. Chromatogr.*, **288**, 451 (1984).
- 19) M. Goto, G. Zou and D. Ishii, *J. Chromatogr.*, **275**, 271 (1983).
- 20) D. Ishii (editor), "Introduction to Microscale High-performance Liquid chromatography", VCH Publishers, New York, 1988, p. 91.
- 21) S. Okuyama, N. Kokubun, S. Higashidate, D. Umemura and Y. Hirata, *Chem. Lett.*, **1979**, 1443.
- 22) D. Ishii, S. Murata and T. Takeuchi, *J. Chromatogr.*, **282**, 569 (1983).
- 23) T. Takeuchi, M. Yamazaki and D. Ishii, *J. Chromatogr.*, **295**, 333 (1984).
- 24) D. W. Armstrong and W. DeMond, *J. Chromatogr. Sci.*, **22**, 411 (1984).
- 25) T. Takeuchi, H. Asai and D. Ishii, *J. Chromatogr.*, **357**, 409 (1986).
- 26) N. Nimura and T. Kinoshita, *J. Chromatogr.*, **352**, 169 (1986).
- 27) T. Takeuchi, T. Niwa and D. Ishii, *J. High Resolut. Chromatogr. Chromatogr. Commun.*, **11**, 343 (1988).
- 28) J.C. Gluckman, A. Hirose, V.L. McGuffin and M.V. Novotny, *Chromatographia*, **17**, **303** (1983).
- 29) T. Takeuchi, T. Saito and D. Ishii, *J. Chromatogr.*, **351**, 295 (1986).
- 30) A. Hirose and D. Ishii, *J. Chromatogr.*, **411**, 221 (1987).
- 31) A. Hirose and D. Ishii, *J. High Resolut. Chromatogr. Chromatogr. Commun.*, **10**, 360 (1987).
- 32) A. Hirose and D. Ishii, *J. Chromatogr.*, **438**, 15 (1988).
- 33) T. Takeuchi, D. Ishii and S. Mori, *J. Chromatogr.*, **257**, 327 (1983).
- 34) T. Takeuchi and D. Ishii, *J. High Resolut. Chromatogr. Chromatogr. Commun.*, **6**, 310 (1983).
- 35) A. Nakanishi, D. Ishii and T. Takeuchi, *J. Chromatogr.*, **291**, 398 (1984).
- 36) D. Ishii, M. Goto and T. Takeuchi, *J. Chromatogr.*, **316**, 441 (1984).
- 37) D.J. Surman and J.C. Vickerman, *J. Chem. Soc., Chem. Commun.*, 1981, 324.
- 38) M. Barber, R.S. Bordoli, R.D. Sedgwick and A.N. Tyler, *J. Chem. Soc. Chem. Commun.*, 1981, 325.
- 39) J.G. Stroh, J.C. Cook, R.M. Milberg, L. Brayton, T. Kihara, Z. Huang and K.L. Rinehart, Jr., *Anal. Chem.*, **57**, 985 (1985).
- 40) Y. Ito, T. Takeuchi, D. Ishii and M. Goto, *J. Chromatogr.*, **346**, 161 (1985).
- 41) R.M. Caprioli and T. Fan, *Anal. Chem.*, **58**, 2949 (1986).
- 42) T. Takeuchi, S. Watanabe, N. Kondo, D. Ishii and M. Goto, *J. Chromatogr.*, **435** 482 (1988).
- 43) Y. Ito, T. Takeuchi, D. Ishii, M. Goto and T. Mizuno, *J. Chromatogr.*, **358**, 201 (1986).
- 44) Y. Ito, T. Takeuchi, D. Ishii, M. Goto and T. Mizuno, *J. Chromatogr.*, **391**, 296 (1987).
- 45) R.M. Caprioli and T. Fan, *Biochem. Biophys. Res. Commun.*, **141**, 1058 (1986).
- 46) R.M. Caprioli, B. DaGue, T. Fan and W.T. Moore, *Biochem. Biophys. Res. Commun.*, **146**, 291 (1987).
- 47) A.E. Ashrott, J.R. Chapman and J.S. Cottrell, *J. Chromatogr.*, **394**, 15 (1987).
- 48) T. Takeuchi, S. Watanabe, N. Kondo, M. Goto and D. Ishii, *Chromatographia*, **25**, 523 (1988).
- 49) F.J. Yang, *J. High Resolut. Chromatogr. Chromatogr. Commun.*, **3**, 589 (1980).
- 50) F.J. Yang, *J. High Resolut. Chromatogr. Chromatogr. Commun.*, **4**, 83 (1981).
- 51) T. Takeuchi and D. Ishii, *J. Chromatogr.*, **435**, 319 (1988).
- 52) T. Takeuchi, T. Asano and D. Ishii, *J. Chromatogr.*, **471**, 297 (1989).
- 53) T. Takeuchi and D. Ishii, *Chromatographia*, **25**, 697 (1988).
- 54) T. Takeuchi and E.S. Yeung, *J. Chromatogr.*, **389**, 3 (1987).
- 55) G. Schill and J. Crommen, *Trends Anal. Chem.*, **6**, 111 (1987).
- 56) H. Small and T. E. Miller, Jr., *Anal. Chem.* **54**, 462 (1982).
- 57) D. Ishii and T. Takeuchi, *J. Liq. Chromatogr.*, **11**, 1865 (1988).
- 58) T. Takeuchi and D. Ishii, *J. Chromatogr.*, **396**, 149 (1987).
- 59) T. Takeuchi, S. Watanabe, K. Murase and D. Ishii, *Chromatographia*, **25**, 107 (1988).
- 60) H.W. Frijlink, J. Visser and B.F.H. Drenth, *J. Chromatogr.*, **415**, 325 (1987).
- 61) T. Takeuchi, M. Murayama and D. Ishii, *J. Chromatogr.*, **477**, 147 (1989).
- 62) S.W. Downey and G.M. Hieftje, *Anal. Chim. Acta*, **153**, 1 (1983).
- 63) T. Takeuchi, E. Suzuki and D. Ishii, *Chromatographia*, **25**, 582 (1988).
- 64) L.J. Galante and G.M. Hieftje, *Anal. Chem.*, **60**, 995 (1988).
- 65) M.J.E. Golay, *Anal. Chem.*, **29**, 928 (1957).

- 66) M.J.E. Golay, *Nature*, **180**, 435 (1957).
- 67) M.J.E. Golay, In "Gas Chromatography 1958", D.H. Desty (editor), Butterworths, London, 1958, p. 36.
- 68) C.G. Horváth, B.A. Preiss and S.R. Lipsky, *Anal. chem.*, **39**, 1422 (1967).
- 69) G. Nota, G. Marino, V. Buonocore and A. Ballio, *J. Chromatogr.*, **46**, 103 (1970).
- 70) K. Hibi, D. Ishii, I. Fujishima, T. Takeuchi and T. Nakanishi, *J. High Resolut. Chromatogr. Chromatogr. Commun.*, **1**, 21 (1978).
- 71) J.W. Jorgenson and E.J. Guthrie, *J. Chromatogr.*, **255**, 335 (1983).
- 72) D. Ishii and T. Takeuchi, *J. Chromatogr. Sci.*, **22**, 400 (1984).
- 73) D. Ishii and T. Takeuchi, In "Advances in Chromatography", J.C. Giddings, E. Grushka, J. Cazes and P.R. Brown (editors), Marcel Dekker, New York, 1983, Vol. 21, p. 131.
- 74) T. Takeuchi and D. Ishii, *J. Chromatogr.*, **240**, 51 (1982).
- 75) T. Takeuchi and D. Ishii, *J. Chromatogr.*, **279**, 439 (1983).
- 76) D. Ishii, T. Niwa, K. Ohta and T. Takeuchi, *J. High Resolut. Chromatogr. Chromatogr. Commun.*, **11**, 800 (1988).
- 77) D. Ishii and T. Takeuchi, *J. Chromatogr. Sci.*, **27**, 71 (1989).
- 78) T. Takeuchi, T. Hamanaka and D. Ishii, *Chromatographia*, **25**, 993 (1988).
- 79) T. Takeuchi, K. Ohta and D. Ishii, *Chromatographia*, **27**, 182 (1989).
- 80) T. Takeuchi, T. Niwa and D. Ishii, *Chromatographia*, **25**, 332 (1988).